File Cy

BRL MR 2724

BRL

MEMORANDUM REPORT NO. 2724

(Supersedes IMR No. 105)

A MODIFIED PRESSURE-IMPULSE BLAST DAMAGE MODEL

R. N. Schumacher
B. E. Cummings

January 1977

USA BALLISTIC RESEARCH LABORATORIES
ABERDEEN PROVING GROUND, MARYLAND

Destroy this report when it is no longer needed.
Do not return it to the originator.

Secondary distribution of this report by originating or sponsoring activity is prohibited.

Additional copies of this report may be obtained from the National Technical Information Service, U.S. Department of Commerce, Springfield, Virginia 22151.

The findings in this report are not to be construed as an official Department of the Army position, unless so designated by other authorized documents.

REPORT DOCUMENTATION PAGE

READ INSTRUCTIONS BEFORE COMPLETING FORM

1. REPORT NUMBER: BRL Memorandum Report No. 2724	2. GOVT ACCESSION NO.
3. RECIPIENT'S CATALOG NUMBER	
4. TITLE (and Subtitle): A MODIFIED PRESSURE-IMPULSE BLAST DAMAGE MODEL	5. TYPE OF REPORT & PERIOD COVERED: FINAL
6. PERFORMING ORG. REPORT NUMBER	
7. AUTHOR(s): R. N. Schumacher B. E. Cummings	8. CONTRACT OR GRANT NUMBER(s)
9. PERFORMING ORGANIZATION NAME AND ADDRESS: USA Ballistic Research Laboratory Aberdeen Proving Ground, MD 21005	10. PROGRAM ELEMENT, PROJECT, TASK AREA & WORK UNIT NUMBERS: 1L662618AH80
11. CONTROLLING OFFICE NAME AND ADDRESS: US Army Materiel Development and Readiness Command 5001 Eisenhower Avenue Alexandria, Virginia 22333	12. REPORT DATE: JANUARY 1977 13. NUMBER OF PAGES: 63
14. MONITORING AGENCY NAME & ADDRESS (if different from Controlling Office)	15. SECURITY CLASS. (of this report): UNCLASSIFIED 15a. DECLASSIFICATION/DOWNGRADING SCHEDULE

16. DISTRIBUTION STATEMENT (of this Report)

Approved for public release; distribution unlimited.

17. DISTRIBUTION STATEMENT (of the abstract entered in Block 20, if different from Report)

18. SUPPLEMENTARY NOTES

This report supersedes BRL Interim Memorandum Report No. 105.

19. KEY WORDS (Continue on reverse side if necessary and identify by block number)

Computer Simulation
Iso-Damage Modeling
Structural Damage Modeling
Overpressure
Blast Damage

20. ABSTRACT (Continue on reverse side if necessary and identify by block number) etm

This report describes the validation of a new analytical technique which relates blast time histories to empirically determined structural damage levels. Its basis lies in two concepts:

(1) Pressure-impulse iso-damage criteria.

(2) Youngdahl's characterization of inelastic structural response in time integrals of loading.

Continued

20. (Continued)

The technique applies to, and relates to, damage done by HE or nuclear blast and damage done by FAE. It minimizes the problem of relating theoretical blast time histories to their empirical counterparts. Its application provides an indepth physical explanation for the relation between cube root charge weight/radius scaling laws and the O. T. Johnson damage scaling law. Application of the proposed analysis model to digital simulations of structural response confirms that time history loading effects may be characterized in a two-parameter set.

TABLE OF CONTENTS

LIST OF ILLUSTRATIONS

LIST OF ILLUSTRATIONS (Continued)

LIST OF TABLES

I. INTRODUCTION

Blast loading phenomena are major contributors to both engineering and military operational environments. Scientific interest was evident as early as the nineteenth century[1,2]. The continuing effort to characterize these phenomenological effects on structures, humans, and military targets includes the work of Sperrazza[3], and O. T. Johnson[4], and Baker[1]. As a continuing part of this effort the current authors propose a model for evaluation of blast-target interaction. The work of several predecessors at the Ballistic Research Laboratories has been influential in forming the proposed model. Consequently, the present report forms a kind of status report on blast vulnerability modeling within the US Army's Ballistic Research Laboratories.

The first concept contributing to the current work is an iso-damage model using a target, a damage level, a blast pressure, and a total blast impulse to characterize blast effects[3].

The second contributing analysis is the work of Youngdahl[5] in which it was found that for rigid-plastic structures, subjected to transient loading, the extent of damage could be characterized by a two parameter set, i.e., those of total impulse and a characteristic time. Both are integrals of load data. This was an important achievement and an indication that similar methods should yield similar results for the blast iso-damage problem.

An important third contribution to the authors' thinking was the blast damage scaling of O. T. Johnson[4]. That approach proposed that level of damage, target and explosive source should combine to define a unique scaling law for blast damage.

In this work the objectives of the authors were to: (1) minimize subjectivity of blast/damage relationships; (2) to simplify data reduction; and (3) to improve accuracy of blast damage analysis. The

---

[1] *Wilfred E. Baker, Explosions in Air, Univ. of Texas Press, Austin, Texas, 1973.*

[2] *F. B. Porzel, "Introduction To A Unified Theory of Explosions (UTE)," NOL TR-72-209, 14 September 1972, Unclassified.*

[3] *J. Sperrazza, "Dependence of External Blast Damage to the A-25 Aircraft on Peak Pressure and Impulse," Ballistic Research Laboratories Memorandum Report 575, September 1951, AD # 378275.*

[4] *O. T. Johnson, "A Blast-Damage Relationship," Ballistic Research Laboratories Report No. 1389, September 1967, AD # 388909.*

[5] *C. K. Youngdahl, "Correlation Parameters for Eliminating the Effect of Pulse Shape on Dynamic Plastic Deformation," Journal of Applied Mechanics, pp. 744-752, September 1970.*

roles of the prior works cited have been to provide a basic model (pressure and impulse*), to provide an additional analysis tool (impulse and a kind of moment integral), and, to provide a means of validation of the process (the O. T. Johnson scaling law). In presenting this work the proposed model is first defined and then related to previous models. Subsequently, it is applied (along with the traditional P-I model) to numerical simulations of the blast/damage process. The authors believe that the results justify wide application of the current model.

II. DESCRIPTION OF THE MODEL

The proposed model is this:

1. Total impulse per unit area delivered by the blast is defined by

$$I_{total} \triangleq \int_{t=0}^{t=t_+} P(t)dt \tag{1}$$

where time starts at load arrival and stops at the end of positive pressure phase, (t_+) while P(t) is the pressure delivered at the target.

2. Two numbers, representing idealized static and impulsive load asymptotes, which cause a specified level of damage, are defined as the critical pressure (P_{cr}) and critical total impulse (I_{cr}).

3. A modified pressure is defined by the integral expression

$$\bar{P} \triangleq \frac{\left(\int_{t_{start}}^{t_{stop}} P(t)dt\right)^2}{2\int_{t_{start}}^{t_{stop}} (t - t_{start})P(t)dt} \tag{2}$$

where t_{start} is the time that P(t) first exceeds P_{cr} and t_{stop} is the time that P(t) drops below P_{cr} (see Figure 1).

4. The fundamental blast/damage model is expressed in the form

Impulse in this report is impulse per unit area unless stated otherwise.

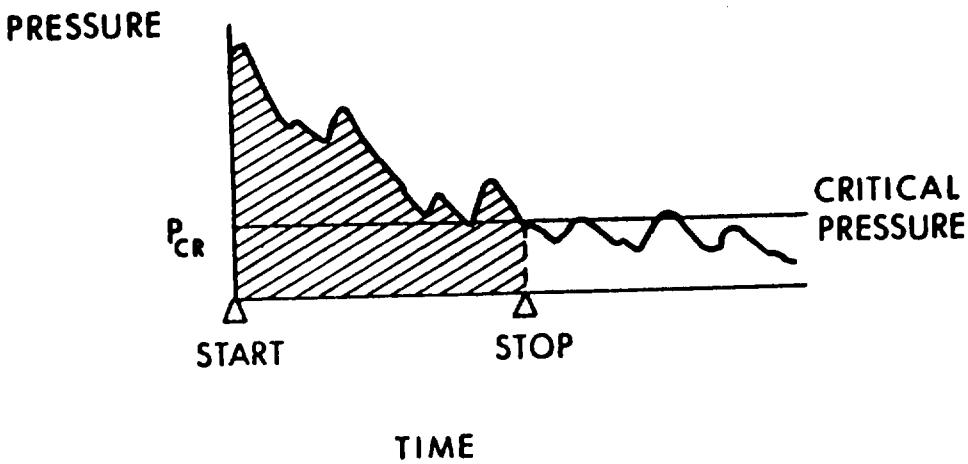

Figure 1. Critical Pressure and Time Criteria of Proposed Model.

$$(\bar{P} - P_{cr})(I_{total} - I_{cr}) = \text{CONSTANT} \quad (3)$$

5. The proposed model may be used when there is no target data (i.e., when P_{cr} and I_{cr} are not known) to evaluate relative blast/damage potential by writing equation (3), with $P_{cr} = I_{cr} = 0$, as

$$\bar{P} \cdot I_{total} \triangleq DN \quad (4)$$

where DN stands for "damage number," a characteristic of the blast pressure only.

Discussion of the model in this report is directed toward those levels of sophistication which the authors believe justified by the past and current practices of the military community. There is no effort to place the presentation in the context found in the physical science studies of blast phenomenology.

III. THE MODEL AND PRIOR WORK

The work of Sperrazza[3] may be characterized by definition of an iso-damage criteria (see Figure 2)

$$(P_p - P_{cr})(I_{total} - I_{cr}) = \text{CONSTANT} \quad (5)$$

where P_p is peak pressure and the subscript cr identifies target characteristics of damage. Equations (3) and (5) are of exactly the same form and only the peak pressure of equation (5) differs from the modified pressure of equation (3). Equation (5), i.e., the historical method, carries an implicit assumption that the pressure time history P(t) has the form

$$P(t) = P_p \phi(t,x,y,z, \ldots) \quad (6)$$

hence for all conditions of nature ϕ has little influence in characterizing failure. That implicit assumption has been very successful in the hands of experienced blast vulnerability analysts. It has also given rise to some difficulty in relating test data to ideal theoretical cases and has made comparison of significantly different types of blast loading difficult (e.g. Pentolite versus Fuel-Air Explosive). It has presented a source of error in data reduction due to the need for subjective selection of peak pressure. It is in removing this technical problem that the work of Youngdahl[5] provides guidance.

Youngdahl proposed the use of a two parameter set to characterize the damage process for a rigid perfectly-plastic target subjected to transient loading. Like Sperrazza he uses total impulse as one parameter. But, instead of peak pressure he uses a characteristic time,

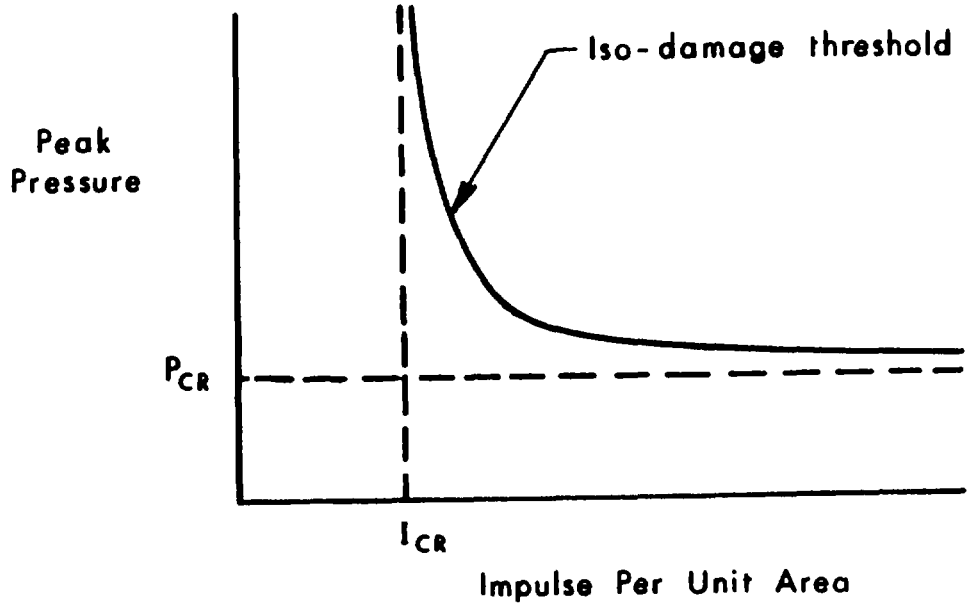

Figure 2. Pressure-Impulse Iso-Damage Model.

$\bar{t}$, defined by

$$\bar{t} \triangleq \frac{2\int_{t_{st}}^{t_{sp}} (t - t_{st})P(t)dt}{\int_{t_{st}}^{t_{sp}} P(t)dt} \tag{7}$$

where t_{st} is the time at which damage starts and t_{sp} is the time at which damage stops (see Figure 3). Note that equation (7) is a normalized first moment of the loading. Given that the procedures for blast damage analysis in the military community already provide for use of the form of equation (5), it is desirable to convert equation (7) into a modified pressure rather than a time. This was done by defining

$$\bar{P} \triangleq \bar{I}/\bar{t} \tag{8}$$

where

$$\bar{I} \triangleq \int_{t_{st}}^{t_{sp}} P(t)dt \quad . \tag{9}$$

The result of substituting equations (7) and (9) into equation (8) is similar in form to that stated in equation (2) where t_{st} is approximated by t_{start} and t_{sp} is approximated by t_{stop}. The consequence of equation (2) (and equation (8)) is that the number pair I_{total} and $\bar{P}$ is obtained without subjective judgement. Caution must be exercised when attempting to analyze data when the function P(t) repeatedly changes sign, because equation (1) implies the P-I relationship applies only for pressure pulses during the first positive overpressure phase. In general, multiple zero pressure crossings of the loading function would indicate a repetitive loading or quasi-steady state forced vibration problem rather than a pulse loading situation to which the P-I technique should be limited.

IV. DISCUSSION OF THE DAMAGE NUMBER MODEL

Equation (4) is the form in which the proposed model must be used when $P_{cr} = I_{cr} = 0$. This also implies that $t_{start} = 0$ and $t_{stop} =$

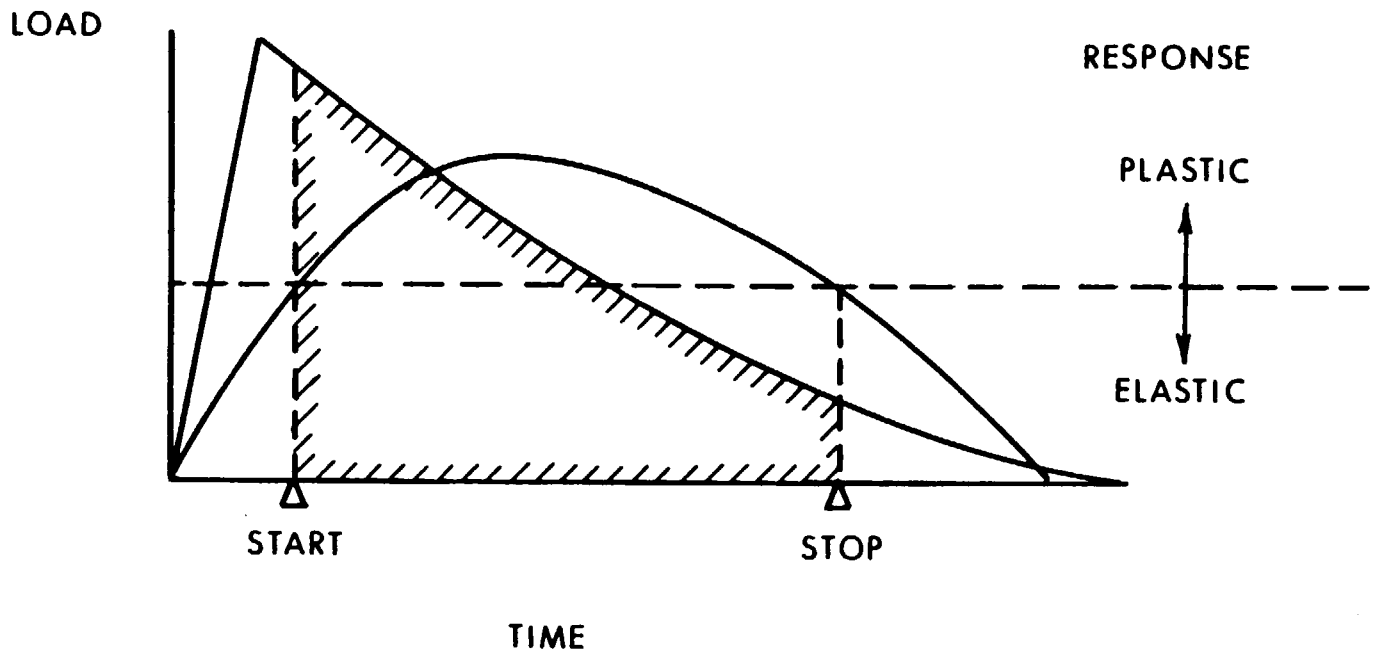

Figure 3. Representation of Youngdahl's Model.

t_+, i.e., that all of the positive pressure history is used to compute $\overline{P}$, because the starting and stopping times for the integrals used to compute $\overline{P}$ are associated with the damage pressure threshold (P_{cr}). We must now refer to the work of O. T. Johnson[4] to establish the relative validity of equation (4).

O. T. Johnson's work relates a normalized nondimensional distance at which a given level of damage can occur (represented in Figure 4 by C_w, a factor inversely proportional to range) to the quantity of explosive used. As is clear from Figure 4, many datum points confirm a scaling law with a slope in the log-log plot equal to 0.435. In Figure 5 a comparison is made between Johnson's predictions and predictions based on the Ballistic Research Laboratory Pentolite data[6] using equation (4). The predictions are based on a reference point for some level of damage (triangle points in Figure 5) having known characteristics of explosive charge mass and standoff distance (range). For the four reference points in Figure 5 predictions were made for the range associated with a charge mass of 100 kg and slopes (in the log-log plot) for the DN = constant predictions determined. The mean value of the DN slopes obtained in Figure 5 is 0.442 which is within one-third of one standard deviation of that obtained by Johnson. The author's interpret the agreement between Johnson's prediction and the DN prediction to be a form of validation of equation (4), the least sophisticated form of the proposed model, with the Ballistic Research Laboratory experimental data base.

The way in which the side-on pressure and reflected pressure bracket Johnson's data (see 100 kg in Figure 5) gives an indication of why subjective estimates of damage can be insensitive to details of the damage mode. Clearly the scaling laws for both side-on and reflected pressure have very similar forms, with only the initial scale requiring adjustment.

V. STATIC LOADS AND IDEAL IMPULSIVE LOADS

The idealized limit cases in which engineering load analysis are imbedded are the static load and the pure impulse ($P(t) \to \infty$, duration $\to 0$). There is no conceptual difficulty in applying equations (1) and (2) to static loading, but for purely impulsive loading some doubt arises. If the positive duration approaches zero, then $\overline{P}$ may not be defined. A careful examination of the application of equations (1) and (2) to a single degree of freedom oscillator excited by a Dirac delta function shows that the value of impulse captured is defined but a value for $\overline{P}$ is infinite. This is the expected result and leads to the conclusion that the method has generality. But in order to ensure

---

[6] *H. J. Goodman, "Compiled Free-Air Blast Data on Bare Spherical Pentolite," Ballistic Research Laboratories Report No. 1092, February 1960, AD # 235278.*

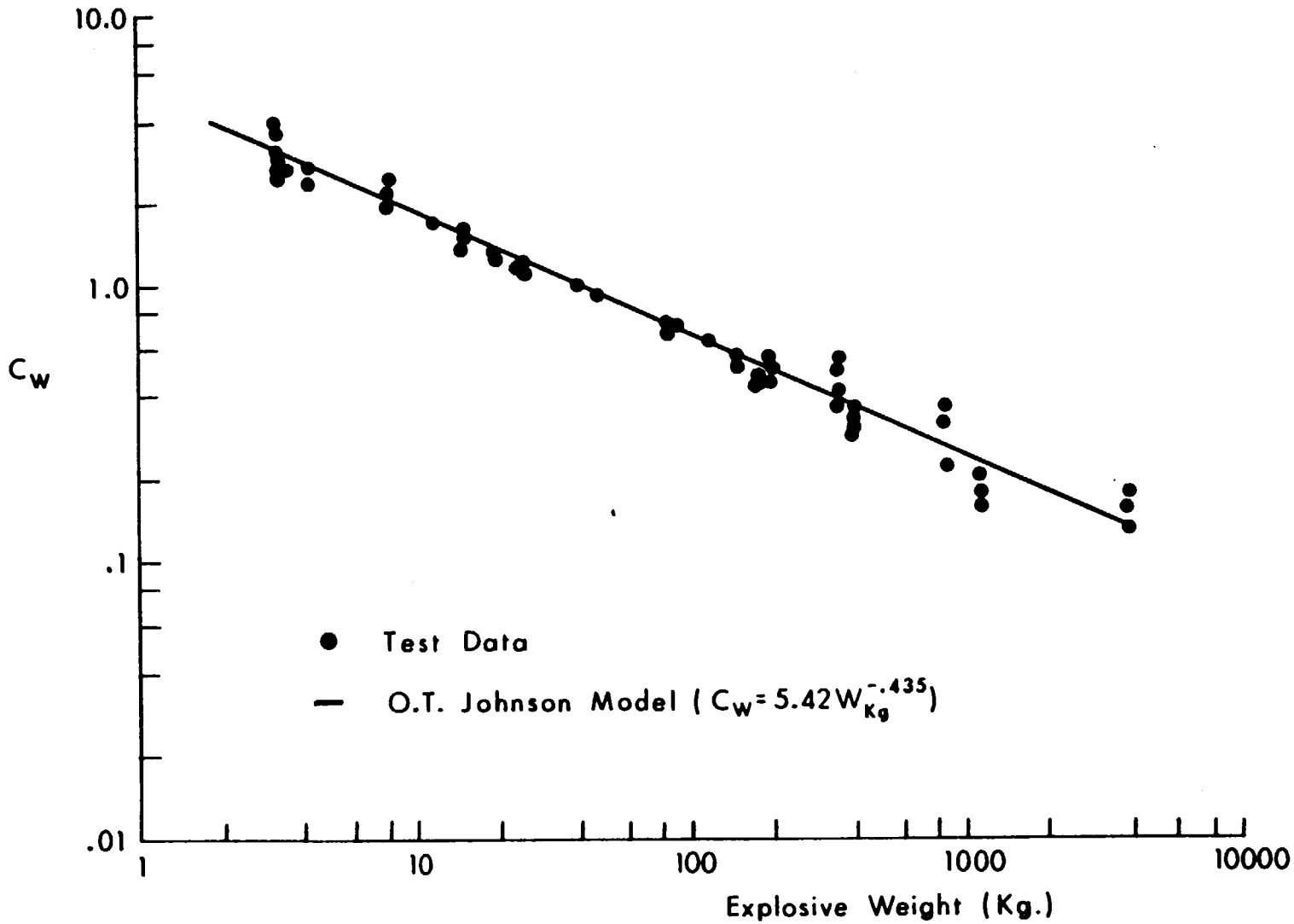

Figure 4. Johnson's Blast Damage Scaling Relationship.

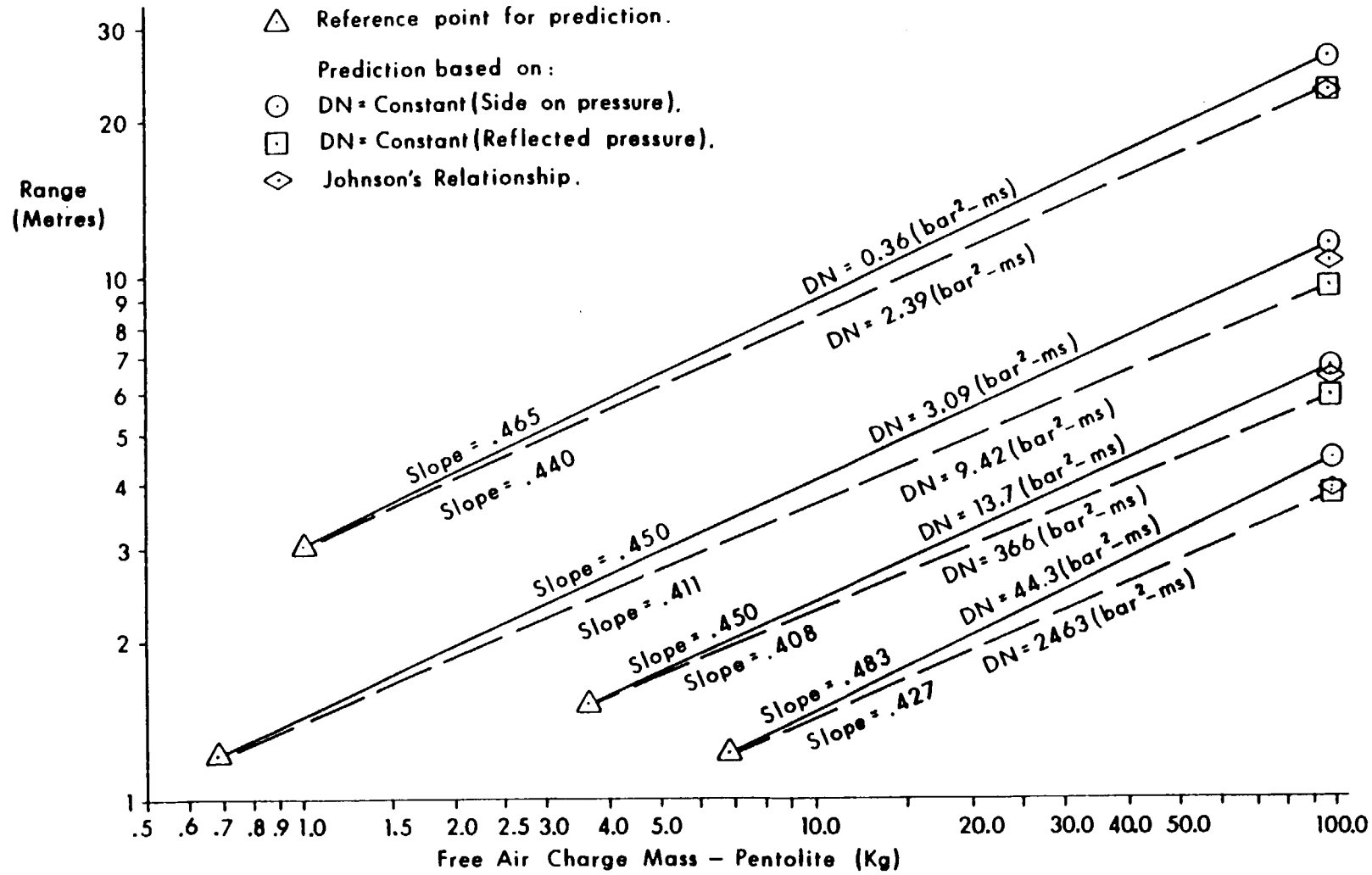

Figure 5. Free-Air Charge Weight Vs. Range for Various Damage Numbers.

greater applicability, the authors have come to the conclusion that the use of the model should probably be restricted to cases where $\overline{P}$ can be calculated directly without access to sophisticated mathematics. As a practical matter, the model is proposed only for those cases where it is possible to determine a critical pressure such that a static pressure of magnitude P_{cr} causes damage equal to that of interest in the blast loaded case. In such cases $\overline{P}$ can always be determined.

VI. CALCULATIONS TO TEST THE MODEL

The concept of the model is of value if it achieves any one of three objectives: (1) that it allows the removal of subjective judgement from blast-damage analysis and testing; (2) that it improves data reduction; or, (3) that it allows data (or analysis) for one class of pressure time histories to predict the blast-damage results of other time histories (i.e., that it removes the problem created by $\emptyset$ of equation (6)).

In order to examine these questions a number of different kinds of loading histories should be examined. Physical experiments have a limited instrumentation capability and even greater limitations of availability. Therefore, it was necessary to augment available test data with computer experiments (i.e., structural response simulations).

Six types of classical pulse loadings were initially considered for this kind of computer experiment: rectangular (flat top, instant rise and fall); quarter cosine (instant rise, cosine fall, no negative phase); linear decay (instant rise, linear fall to zero overpressure); half sine wave (no negative phase); ramp (linear rise, instant fall); and, Friedlander. Figure 6 shows the result of applying equation (2) to the first five types of loading. This figure can be used to determine the pressure ratios that are required to achieve the third objective stated earlier in this section.

Four kinds of computer simulations were used to obtain data on perfectly instrumented targets with which to study the proposed model: single and five degree-of-freedom models; a cylinder model (psuedo-Kirchoff theory); and, an advanced beam vibration model. Figures 7 and 8 depict the kinds of systems simulated by the first two models. Figure 9 depicts the time histories applied to the one and five degree-of-freedom and REPSIL models. Figure 10 shows the shell model with its spacial distribution of load having either rectangular or exponentially decaying time dependent pressure loads. Figures 11 through 14 show the configurations, time histories and load parameters of the advanced beam analysis.

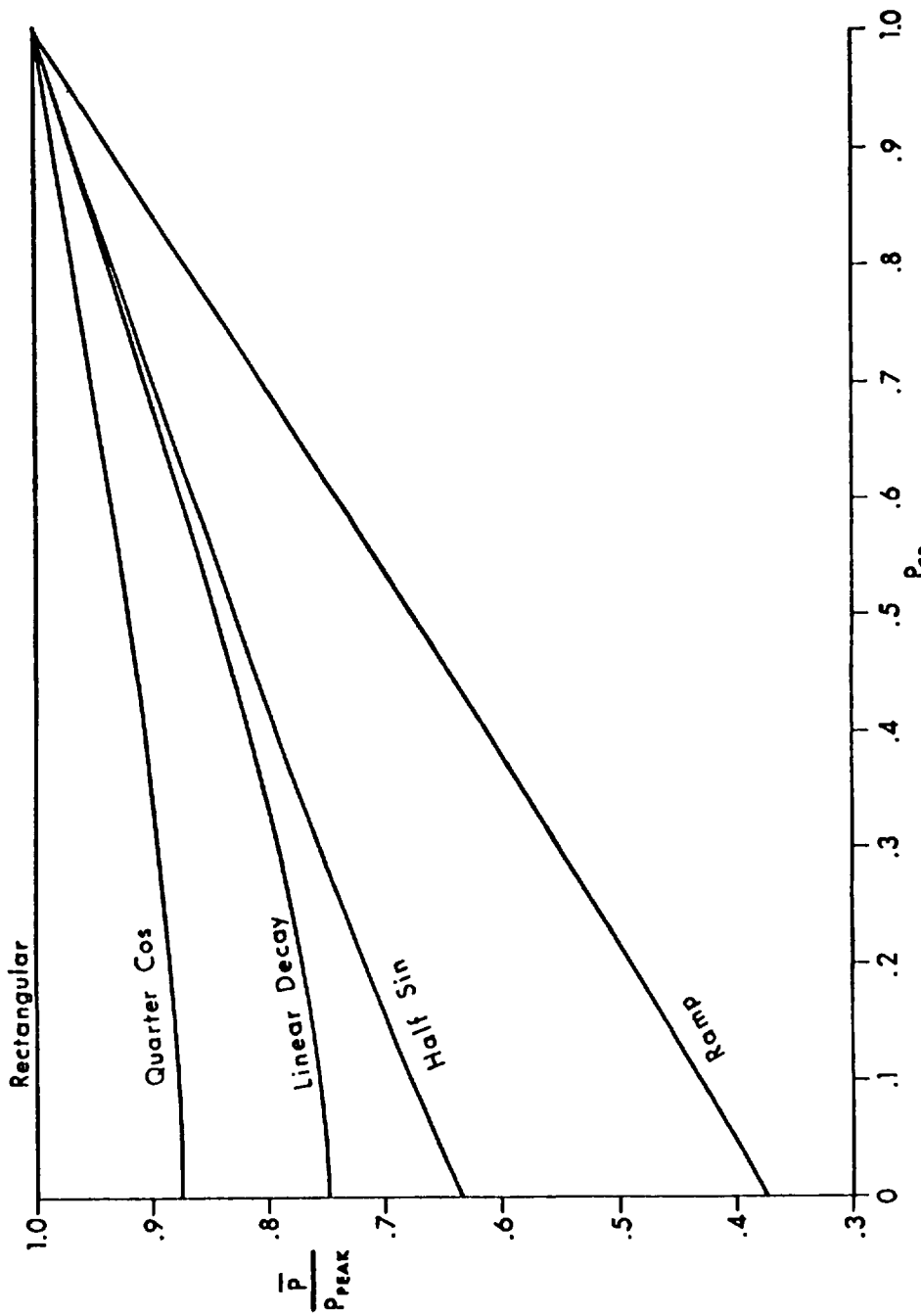

Figure 6. Non-Dimensional Pulse Parameters for the Proposed Model.

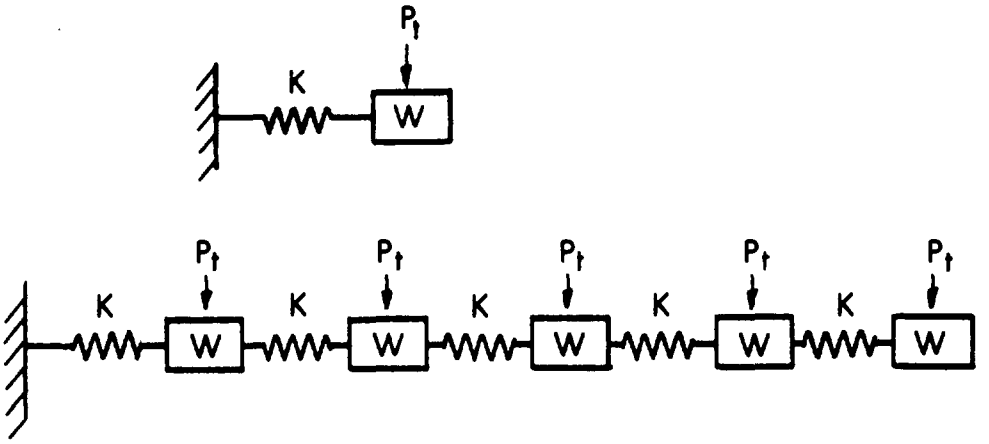

Figure 7. Schematic Representation of SWRI Models Used.

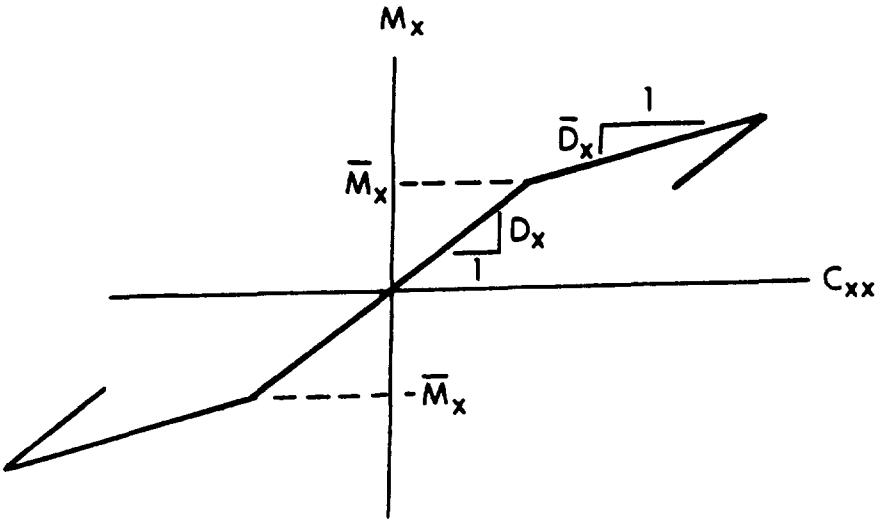

Figure 8. Bilinear Moment - Curvature Relations Used In SWRI Computer Code.

RECTANGULAR PULSE

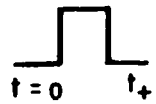

$$P(t) = P_0 \quad \text{for} \quad 0 \leq t \leq t_+$$

LINEAR DECAY PULSE

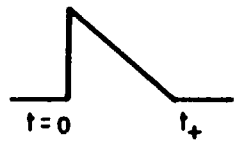

$$P(t) = P_0\left(1 - \frac{t}{t_+}\right) \quad \text{for} \quad 0 \leq t \leq t_+$$

EXPONENTIAL DECAY PULSE

$$P(t) = P_0\left(1 - \frac{t}{t_+}\right) e^{-\beta \frac{t}{t_+}} \quad \text{for} \quad 0 \leq t \leq t_+$$

RAMP PULSE

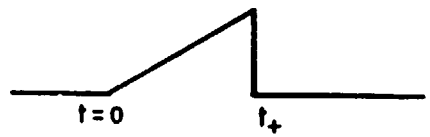

$$P(t) = P_0\left(\frac{t}{t_+}\right) \quad \text{for} \quad 0 \leq t \leq t_+$$

SAW TOOTH PULSE

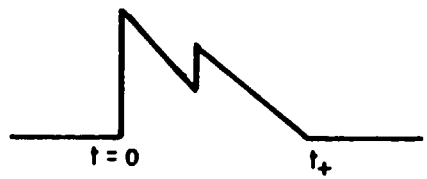

$$P(t) = P_0\left(1 - \frac{1.3t}{t_+}\right) \quad \text{for} \quad 0 \leq t \leq .5t_+$$

$$P(t) = 1.3P_0\left(1 - \frac{t}{t_+}\right) \quad \text{for} \quad .5t_+ \leq t \leq t_+$$

Figure 9. Pressure Loading Functions Used in the SWRI and REPSIL Models.

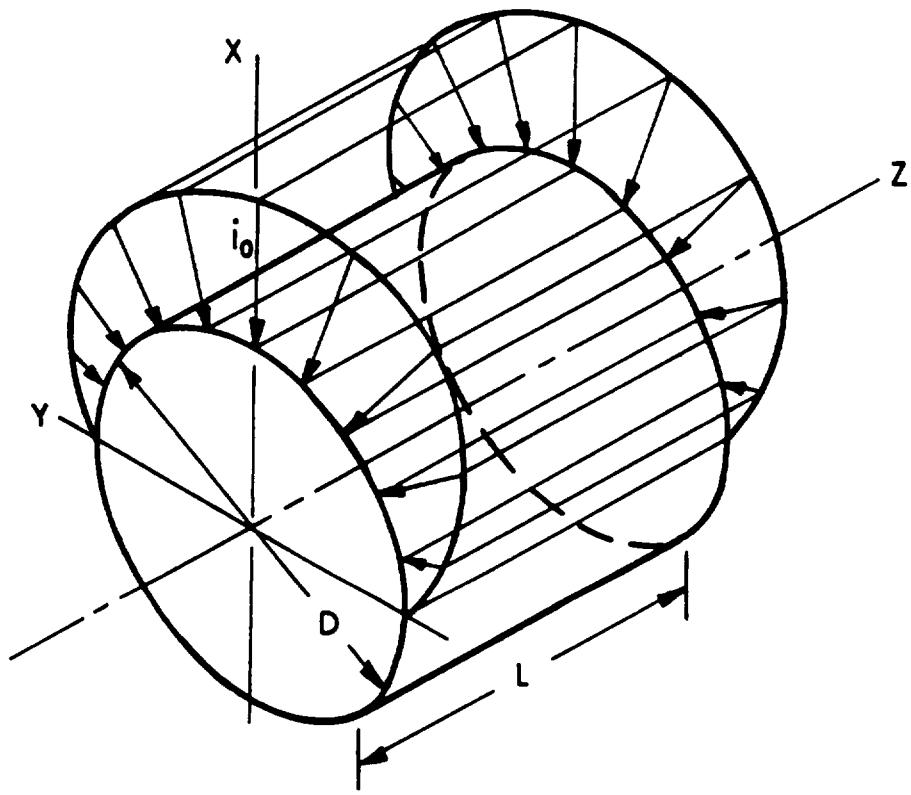

Figure 10. Frontal Cosine Loading of Fixed-Ended Cylinder.

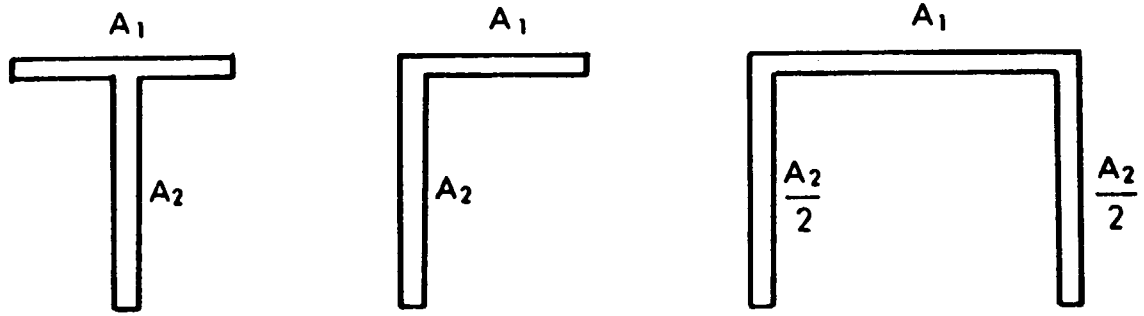

TWO-AREA CROSS SECTIONS

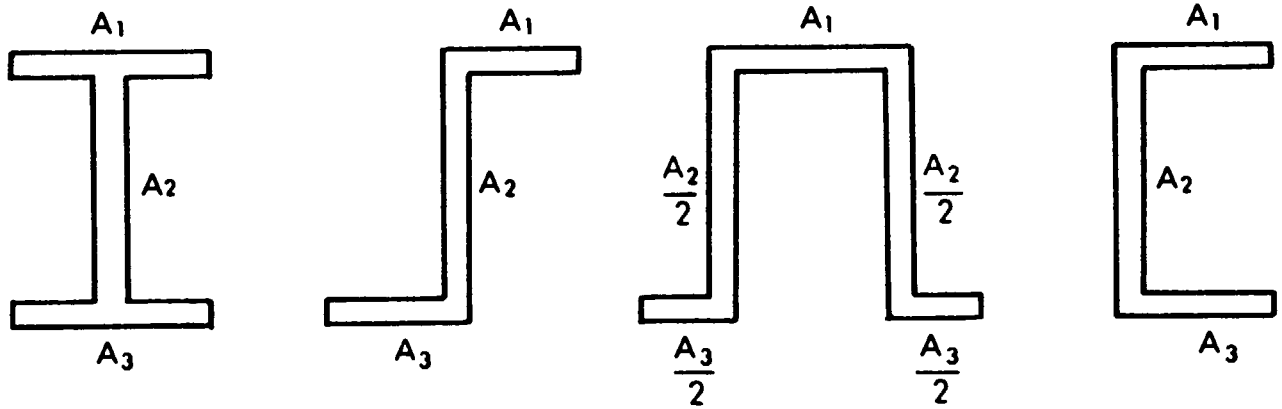

THREE-AREA CROSS SECTIONS

Figure 11. Typical Extrusion Cross-Sections.

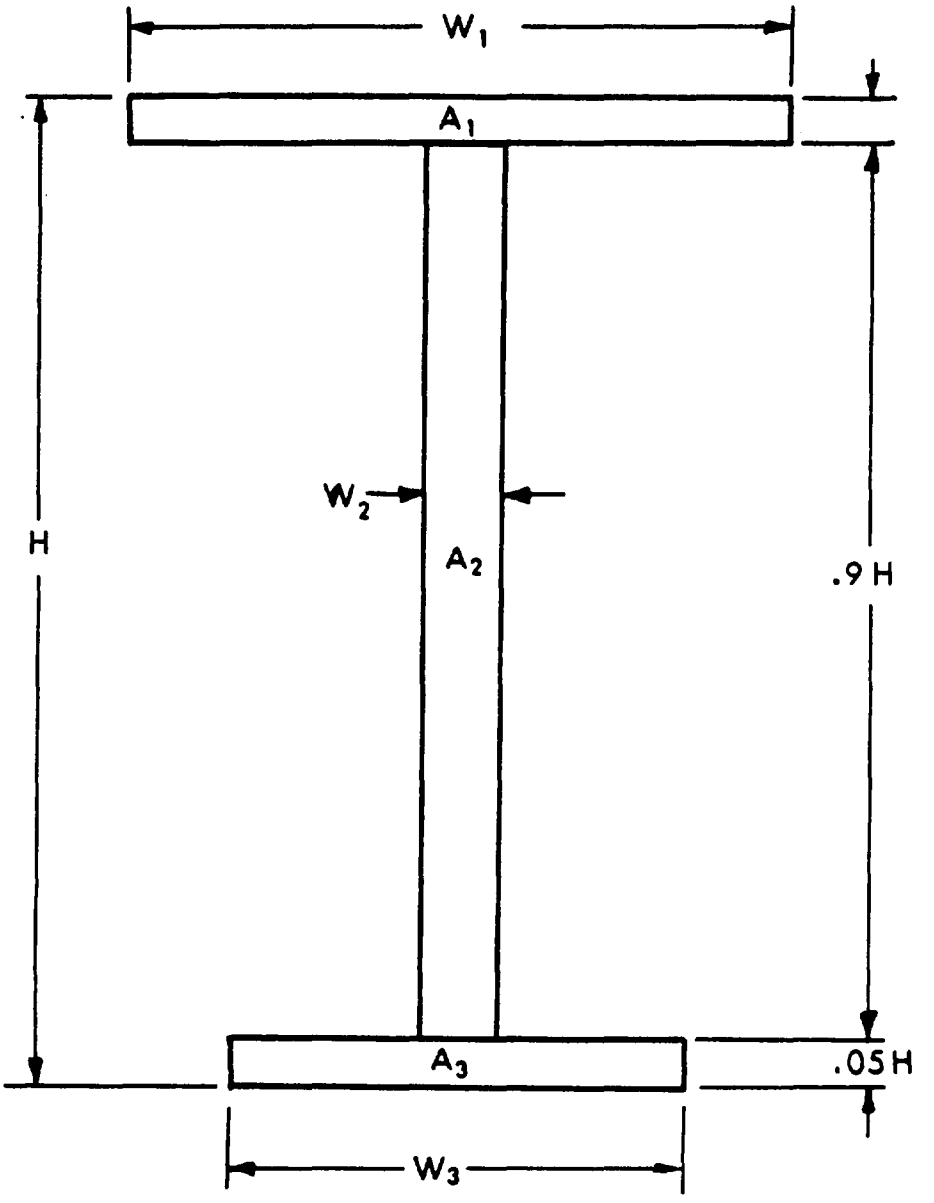

$$\frac{\text{Area } A_2}{\text{Area } A_1} = \frac{.9H\,W_2}{.05H\,W_1} = 18\,\frac{W_2}{W_1}$$

$$\frac{\text{Area } A_3}{\text{Area } A_1} = \frac{.05H\,W_3}{.05H\,W_1} = \frac{W_3}{W_1}$$

Figure 12. Synthesized Beam Cross-Section.

For the single triangle case: use $f_2(t)$ only.

For the exponential case: use $f_1(t)$ only with $n = a = 1$.

For the double triangle case: $a = 0$, $n = 1$

$P_1 = 2P_0$, $t_1 = \frac{t_0}{3}$.

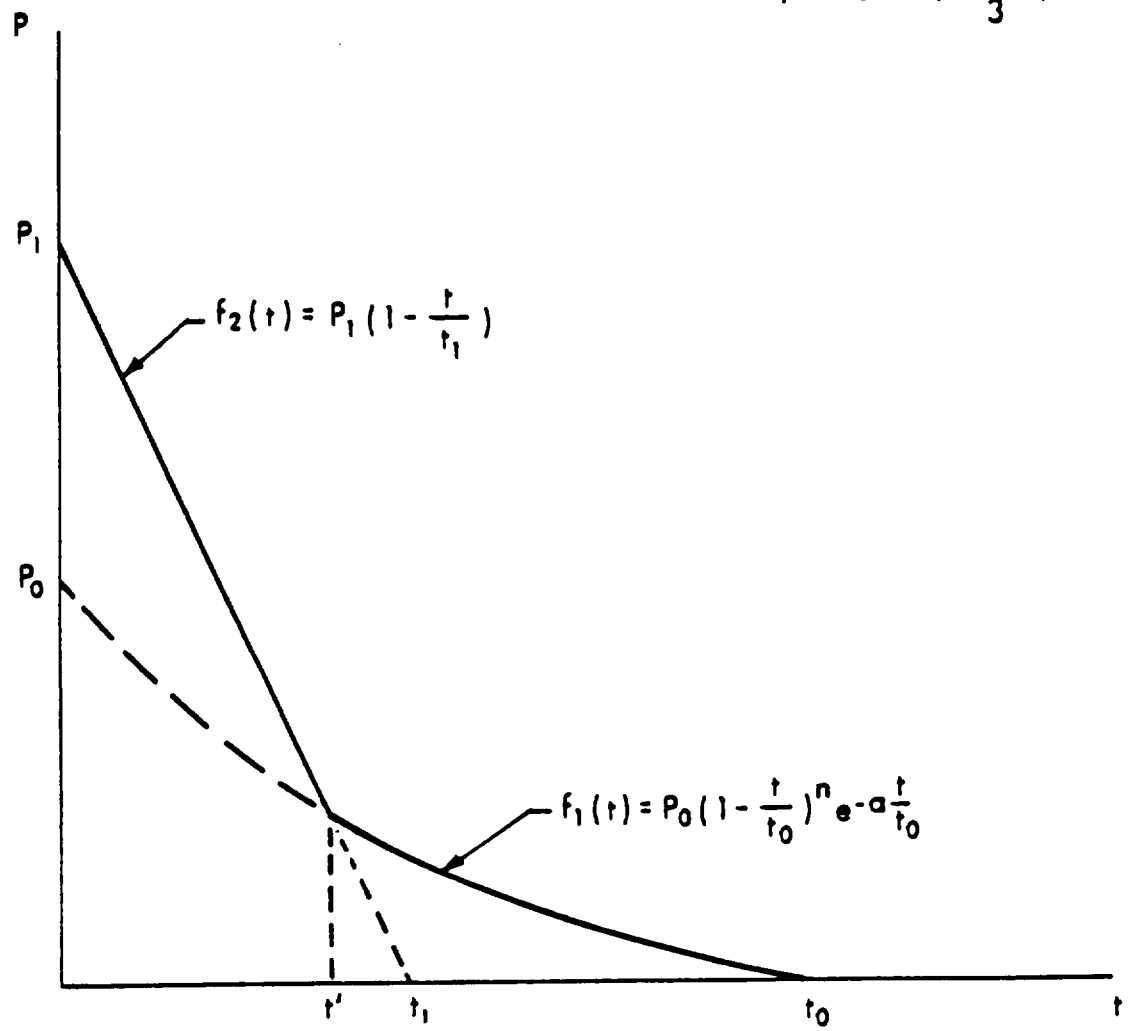

Figure 13. KADBOP Blast Response Code Forcing Functions.

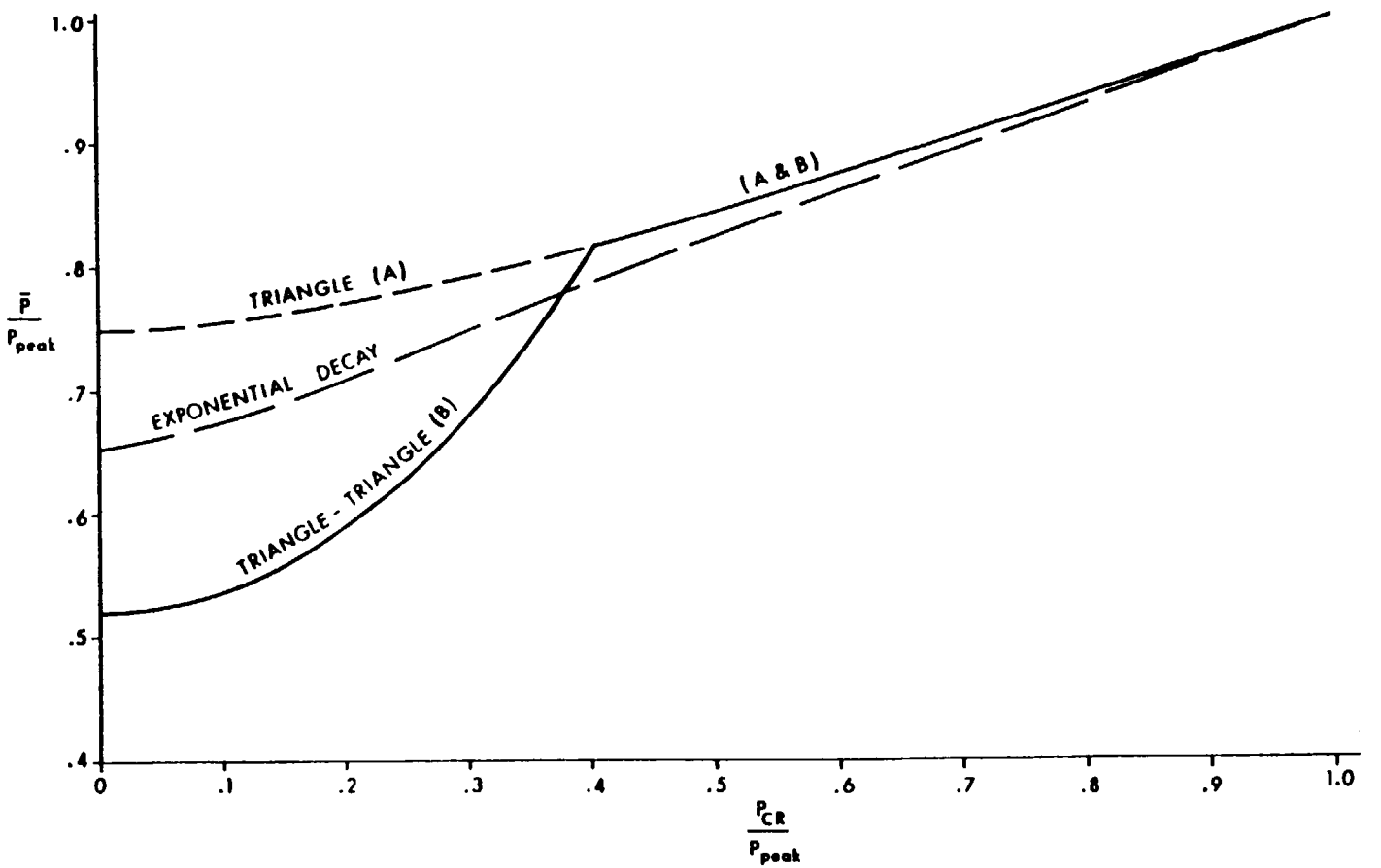

Figure 14. Pulse Parameter Curves for Analysis of Kaman Data.

The analysis of the single degree-of-freedom system and the five degree-of-freedom system were conducted using a finite difference computer code[7] developed by Southwest Research Institute (SWRI) under contract to BRL. In that program the plate (or beam case utilized) equations of motion for flexure are solved under assumed moment-curvature relations. It was assumed that a bilinear moment-curvature relation with hysteretic recovery could approximate the response of a representative system made of aluminum alloy. In Figure 8, D_x is the elastic rigidity, $\bar{D}_x$ is the plastic flexural rigidity and M_x is the bending moment at which the transition occurs.

The schematic form of the first two systems investigated are those shown in Figure 7 where K represents the spring bending characteristics, W represents the mass of each element and P_t represents the blast loading function to be applied to the system. Table I lists the parameters used to analyze those systems.

The output of the computer program was the maximum bending moment obtained in each spring element. Beam curvature is known and, assuming a beam thickness, the resulting maximum strain can be determined after the system is allowed to oscillate through enough cycles to be reasonably assured that the maximum strains were achieved. For the one degree-of-freedom system this occurred on the first cycle of response. However, for the five degree-of-freedom system many cycles were allowed to proceed before stopping.

These two computational experiments were chosen as a means of investigating a wide range of loading characteristics as shown in Figure 9.

The cylindrical shell computation was included in order to take advantage of the highly developed REPSIL[8,9] computer code. The specific case studied is a fixed end 6061-T6 circular cylindrical shell of 768 elements having the properties listed in Table I.

---

[7] *W. E. Baker, S. Silverman, P. A. Cox, Jr., and D. Young, "Structural Response of Helicopters to Muzzle and Breech Blast," Vol II, Final Technical Report SWRI 02-2029, Contract No. DAAD 05-67-C-0201 (BRL) dated March 1962.*

[8] *N. J. Huffington, Jr., "Large Deflection Elastoplastic Response of Shell Structures," Ballistic Research Laboratories Report 1515, November 1970, AD # 717005.*

[9] *N. J. Huffington, Jr., "An Analytical Study of Explosive Loading Techniques for Simulation of Impulsive Loading to Structures at Lethality Levels," Ballistic Research Laboratories Report No. 1621, November 1972, AD # 907436-L.*

Table I. Parameters Used in SWRI and REPSIL Computer Codes.

SWRI One and Five Degree-of-Freedom Beam Parameters

Parameter	1 degree-of-freedom	5 degree-of-freedom
D_x	0.0380 N-m^4 (20500 lb-in^4)	0.0254 N-m^4 (13700 lb-in^4)
$\overline{D}_x$	0.235 mN-m^4 (127 lb-in^4)	0.156 mN-m^4 (84.6 lb-in^4)
M_x	76.5 N-m (677 lb-in)	86.5 N-m (766 lb-in)
W	0.116 kg (0.255 lb)	0.020 kg (0.045 lb)
Beam Thickness	0.95 cm (0.375 in)	0.64 cm (0.250 in)
Element Length	22.86 cm (9.0 in)	4.57 cm (1.8 in)
Element Width	2.54 cm (1.0 in)	2.54 cm (1.0 in)

REPSIL Shell Properties

Property	
Young's Modulus	7.24 x 10^5 bar (10.5 x 10^6 psi)
Poisson's Ratio	1/3
Yield Stress	2896 bar (42,000 psi)
Mass Density	230.7 kg/m^3 (0.000259 lb-s^2/in^4
Length	15.24 cm (6 in)
Nominal O.D.	7.62 cm (3 in)
Thickness	0.107 cm (0.042 in)

The pressure histories applied to the shell act over the top half cylinder having peak pressure on the crown line and a cosine distribution around to the half cylinder line as shown in Figure 10. The time histories have the general form

$$P = \cos\theta \, P_o \, (1 - t/t_+)\exp(-\beta t/t_+) \quad ,$$

where θ is zero at the crown line of the cylinder and $\beta = 2.0$.

The final system considered in the model validation was a contractor effort[10] which was generated under a separate set of requirements. It was included because it provides an example of a relatively heavy beam structure. The relatively stiff structure (clamped at both ends) filled out the spectrum of targets even though the loading was very limited. The degree of limitation on the loading is made clear by examination of Figure 14. The loads are essentially identical over 60 percent of target loading regime.

The contractor calculations were made using their KADBOP[10] code. The KADBOP beam program employs a finite element approach wherein the beam is represented by a series of discrete masses interconnected by straight weightless bars. Fifteen equally spaced mass points were used to simulate the beam length and the beam was assumed to be uniformly loaded.

To use the Kaman data in the correlated concept presented here, it was necessary to re-compute $\bar{P}$. To do this the three curves of Figure 14 were determined for the loading functions used by the contractor to determine non-dimensional forms of the parameters, P_{cr}, P_{peak}, and $\bar{P}$.

VII. CALCULATED TEST RESULTS

To test the results of the model we have: created numerical simulation of physical experiments; applied the model to the results; applied the conventional techniques (peak pressure versus total impulse) to the results; and, examined the relative dispersion of the two methods. Visual (i.e., subjective) judgements are made as to the relative merits of the two methods. A perfect method would produce iso-damage curves that are independent of loading pulse shape. Neither system is perfect, therefore, closeness (minimum distance between) of curves for a given iso-damage criterion with different time histories is our standard of how good a given method is. Only relative measures of goodness are possible in this way.

---

[10] *K. R. Wetmore, "An Interim Technical Report on Phase I of the BRL Pressure Impulse Blast Program," 30 September 1974, Contract DAA05-74-C-0742, Kaman Avidyne.*

It is difficult to give an objective measure for the value of an engineering practice, but the authors believe that the ability to cause all fixed damage iso-damage curves to fall within experimental scatter of one another would meet the third objective stated in Section VI.

In general, an iso-damage criteria is selected to satisfy a "constant level-of-damage requirement." This criteria could have been: maximum strain anywhere in the target, maximum deflection of the target, maximum deflection at a specified location on the target, etc. However, for the purposes of the investigation the iso-damage criteria was arbitrarily selected to be the maximum percent strain on the surface of the target as calculated at the discrete grid locations.

Data about the results is given here in two forms: Tables II through V and, Figures 15 through 24. Tabular data is included because the present evaluation of the proposed model is still subjective. Other investigators may choose to use some traditional objective method of comparing the data for both P-I and $\overline{P}$-I iso-damage methodology. The present authors have sought the assistance of experts within the Ballistic Research Laboratories* to assess the relative merits of the two methods. No technique was immediately available; therefore, the subjective evaluation will be published at this time.

The subjective evaluation used by the authors was based on the question: How well do the iso-damage curves for one loading history (Ø of equation (6)) predict other loadings? Specifically: How well relatively, do the rectangular pulse iso-damage curves (one degree-of-freedom case) in Figures 15 and 16 predict iso-damage data for a linear decay pulse or data for a sawtooth pulse or other type loadings? Similar questions are applied to the five degree-of-freedom simulation data of Figures 17 and 18. For REPSIL the question is how well does rectangular pulse data predict exponential decay data (Figures 19 and 20)? For the Kaman Avidyne beam data we ask the reader to pose his own comparison (Figures 21 through 24). In these last four figures the authors believe that the case is as strongly in favor of the $\overline{P}$-I method as in the preceding cases. However, it has been suggested that merely displaying a curve fit to a part of the data biases the observers' opinion. The Kaman Avidyne data was chosen to be left without a reference curve because it has the least variation in loading function (see Figures 13 and 14) and therefore, subjective judgement of the results was most likely to be biased by introduction of visual reference.

It is the judgement of the authors that visual inspection of Figures 15 through 24 clearly supports the contention that the use of $\overline{P}$ and I is superior to the use of P_{peak} and I. The weakest support

Private communications: Dr. Malcolm Taylor

Table II. Single Degree-of-Freedom Iso-damage Data

Loading Function Type	Strain = 1.5% Average* Pressure $\bar{P}$ (bar)	Peak Pressure P (bar)	Total Impulse I(bar-ms)	Strain = 5.0% Average** Pressure $\bar{P}$ (bar)	Peak Pressure P (bar)	Total Impulse I(bar-ms)	Strain = 9.0% Average*** Pressure $\bar{P}$ (bar)	Peak Pressure P (bar)	Total Impulse I(bar-ms)
rectangular	6.21	6.21	3.79	6.21	6.21	7.75	6.21	6.21	10.4
	3.44	3.44	3.79	3.44	3.44	7.77	2.07	2.07	11.6
	2.07	2.07	3.84	2.07	2.07	8.18	1.39	1.39	12.6
	1.39	1.39	3.90	1.39	1.39	8.72	1.03	1.03	14.1
	1.03	1.03	4.05	1.03	1.03	9.65	0.862	0.862	16.1
	0.689	0.689	4.52	0.862	0.862	10.6			
	0.510	0.510	5.92	0.689	0.689	13.8			
linear decay	3.14	4.14	3.85	3.16	4.14	7.81	3.17	4.14	10.8
	2.12	2.76	3.86	2.14	2.76	8.08	2.15	2.76	11.4
	1.61	2.07	3.91	1.64	2.07	8.46	1.65	2.07	12.0
	1.37	1.73	3.96	1.39	1.73	8.83	1.40	1.73	12.5
	1.12	1.39	4.14	1.14	1.39	9.73	1.15	1.38	13.9
	0.87	1.03	4.66	0.90	1.03	12.5	0.98	1.14	17.2
	0.72	0.834	5.46	0.80	0.89	17.2			
	0.63	0.703	8.29						
	0.53	0.565	17.2						
SAW TOOTH	0.779	1.03	4.83	1.50	2.07	8.88	1.50	2.07	12.7
				1.03	1.38	10.4			

* P_{cr} = 0.503 bar

** P_{cr} = 0.621 bar

*** P_{cr} = 0.652 bar

Table III. Five Degree-of-Freedom Iso-damage Data

Loading Function Type	Strain = 1.5% Average* Pressure $\bar{P}$ (bar)	Strain = 1.5% Peak Pressure P (bar)	Strain = 1.5% Total Impulse I(bar-ms)	Strain = 5.0% Average** Pressure $\bar{P}$ (bar)	Strain = 5.0% Peak Pressure P (bar)	Strain = 5.0% Total Impulse I(bar-ms)	Strain = 9.0% Average*** Pressure $\bar{P}$ (bar)	Strain = 9.0% Peak Pressure P (bar)	Strain = 9.0% Total Impulse I (bar-ms)
	6.21	6.21	2.32				6.21	6.21	7.06
Rectangular	4.83	4.83	2.39	4.83	4.83	5.18	4.83	4.83	7.10
	3.10	3.10	2.59	3.10	3.10	5.31	3.10	3.10	7.34
	2.07	2.07	2.92	2.07	2.07	5.69	2.07	2.07	7.69
	1.38	1.38	3.05	1.38	1.38	6.19	1.65	1.65	8.17
	1.03	1.03	3.35	1.17	1.17	6.89	1.38	1.38	8.80
	0.827	0.827	3.78	1.01	1.01	8.62	1.17	1.17	10.3
	0.738	0.738	5.17	0.972	0.972	10.3	1.05	1.05	13.8
	0.733	0.733	16.9	0.958	0.958	13.8	1.04	1.04	16.9
	0.728	0.728	6.89	0.957	0.957	16.9			
	0.727	0.727	8.62						
	0.725	0.725	10.3						
	0.724	0.724	13.8						
	4.70	6.21	2.48	4.74	6.21	5.12	4.75	6.21	7.00
	3.68	4.83	2.58	3.71	4.83	5.31	3.73	4.83	7.20
	2.15	2.76	3.10	2.20	2.76	5.69	2.23	2.76	7.91
Linear Decay	1.66	2.07	3.38	1.71	2.07	6.40	1.74	2.07	8.96
	1.36	1.65	3.32	1.43	1.65	7.24	1.60	1.87	9.31
	1.17	1.38	3.62	1.41	1.65	7.01	1.39	1.61	12.1
	0.97	1.10	4.22	1.23	1.38	9.31	1.26	1.38	16.5
	0.869	0.951	5.52	1.14	1.25	12.1			
	0.786	0.838	7.24	1.07	1.10	16.5			
	0.759	0.793	12.1						
	0.759	0.789	16.5						
SAW TOOTH	2.45	3.45	3.00	2.48	3.45	5.56	2.49	3.45	7.60
	1.50	2.07	3.36	1.54	2.07	6.56	1.56	2.07	9.27
RAMP	1.94	4.14	2.76	2.06	4.14	5.70	2.16	4.14	7.54
	1.43	2.76	2.97	1.56	2.76	6.00	1.38	2.07	10.55

* P_{cr} = 0.69 bar

** P_{cr} = 0.90 bar

*** P_{cr} = 1.00 bar

Table IV. REPSIL Iso-damage Data

Loading Function Type	Strain = 3.0% Average* Pressure $\bar{P}$ (bar)	Strain = 3.0% Peak Pressure P (bar)	Strain = 3.0% Total Impulse I(bar-ms)	Strain = 5.0% Average* Pressure $\bar{P}$ (bar)	Strain = 5.0% Peak Pressure P (bar)	Strain = 5.0% Total Impulse I(bar-ms)	Strain = 9.0% Average* Pressure $\bar{P}$ (bar)	Strain = 9.0% Peak Pressure P (bar)	Strain = 9.0% Total Impulse I(bar-ms)
Rectangular	345.0	345.0	2.68	345.0	345.0	3.77	345.0	345.0	4.68
	205.0	205.0	2.69	205.0	205.0	3.92	205.0	205.0	4.91
	81.6	81.6	3.25	105.0	105.0	4.41	136.0	136.0	5.36
	61.6	61.6	3.53	84.4	84.4	4.78	104.0	104.0	6.00
Exponential Decay	345.0	580.0	2.60	345.0	580.0	3.84	345.0	580.0	4.77
	143.0	240.0	2.82	192.0	323.0	3.98	246.0	413.0	4.81
	84.4	142.0	3.23	114.0	192.0	4.36	138.0	232.0	5.29
	29.0	38.5	5.87	62.9	106.0	6.09	47.0	79.0	9.38
	18.0	30.3	7.79	39.4	66.2	8.07	29.7	49.9	12.5
	15.9	26.7	8.62	25.6	43.0	11.0	26.3	44.2	13.7
				22.8	38.3	11.9			

* Based on $P_{CR} \approx 0$

Table V. Data from Kaman Avidyne Beam Response Calculations

Loading Function Type	Strain = 3.0% Average* Pressure $\bar{P}$(bar)	Peak Pressure P (bar)	Total Impulse I(bar-ms)	Strain = 15.0% Average** Pressure $\bar{P}$ (bar)	Peak Pressure P (bar)	Total Impulse I(bar-ms)
	5.18	6.46	3.23	18.61	23.46	11.73
	3.44	3.99	3.99	11.01	12.71	12.71
	2.79	3.06	6.13	8.61	9.26	18.52
Triangular	2.58	2.75	8.26	8.09	8.50	25.48
(Linear	2.48	2.61	10.46	7.87	8.15	32.62
Decay)	2.41	2.52	12.59	7.74	7.97	39.83
	2.35	2.42	18.14	7.58	7.73	57.98
	2.32	2.37	23.72	7.49	7.62	76.21
	2.28	2.32	34.89	7.43	7.51	112.6
	2.28	2.30	46.07	7.37	7.45	149.0
	2.26	2.28	79.59	7.32	7.37	258.1
	2.24	2.26	113.20	7.32	7.34	367.3
	6.28	8.60	3.17	23.37	32.59	11.99
	4.05	5.07	3.72	13.29	16.61	12.22
Expo-	3.16	3.67	5.41	9.86	11.26	16.57
nential	2.86	3.21	7.08	8.82	9.66	21.33
Decay	2.68	2.94	8.67	8.39	9.00	26.48
	2.59	2.80	10.30	8.16	8.62	31.72
	2.47	2.61	14.39	7.83	8.14	44.92
	2.40	2.50	18.37	7.69	7.92	58.26
	2.34	2.41	26.57	7.55	7.70	85.03
	2.31	2.37	34.77	7.47	7.59	111.8
	2.27	2.30	59.39	7.38	7.46	191.9
	2.26	2.28	84.00	7.34	7.39	271.9
	6.40	10.66	3.20	23.00	39.45	11.83
	4.68	6.38	3.83	15.34	20.90	12.54
Triangular-	3.87	4.63	5.56	12.40	14.74	17.69
Triangular	3.39	3.95	7.10	10.71	12.36	22.24
(Bilinear	3.10	3.52	8.44	9.61	10.73	25.75
Decay)	2.92	3.25	9.75	8.96	9.79	29.37
	2.66	2.88	12.97	8.30	8.82	39.69
	2.54	2.70	16.19	7.97	8.35	50.08
	2.43	2.53	22.81	7.74	7.97	71.79
	2.39	2.44	31.39	7.61	7.79	93.52
	2.31	2.35	49.39	7.46	7.57	159.0
	2.28	2.32	69.52	7.39	7.48	224.4

* P_{cr} = 2.21 bar

** P_{cr} = 7.24 bar

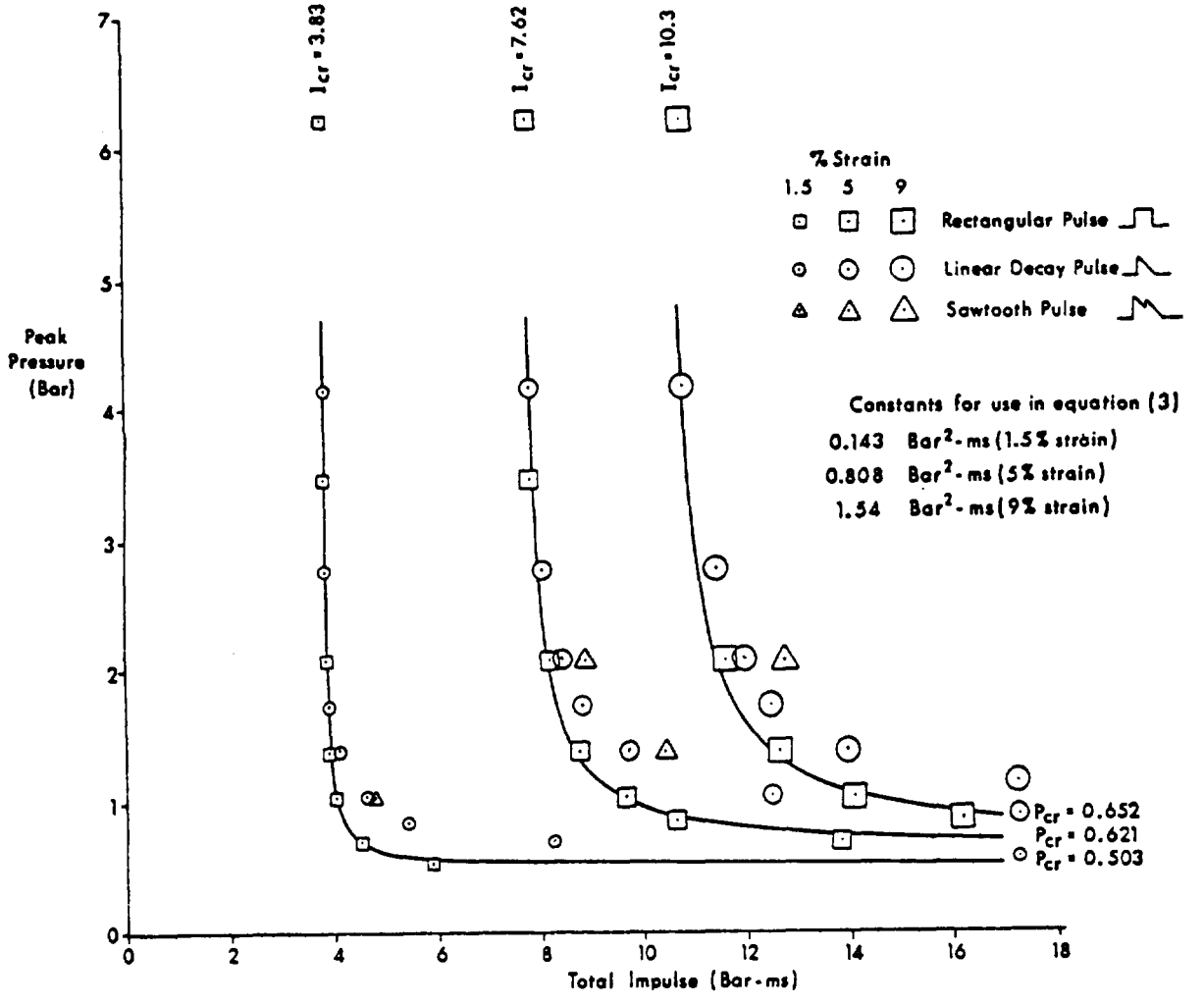

Figure 15. Plot of P_{peak} Vs. Total Impulse for One Degree-of-Freedom Data.

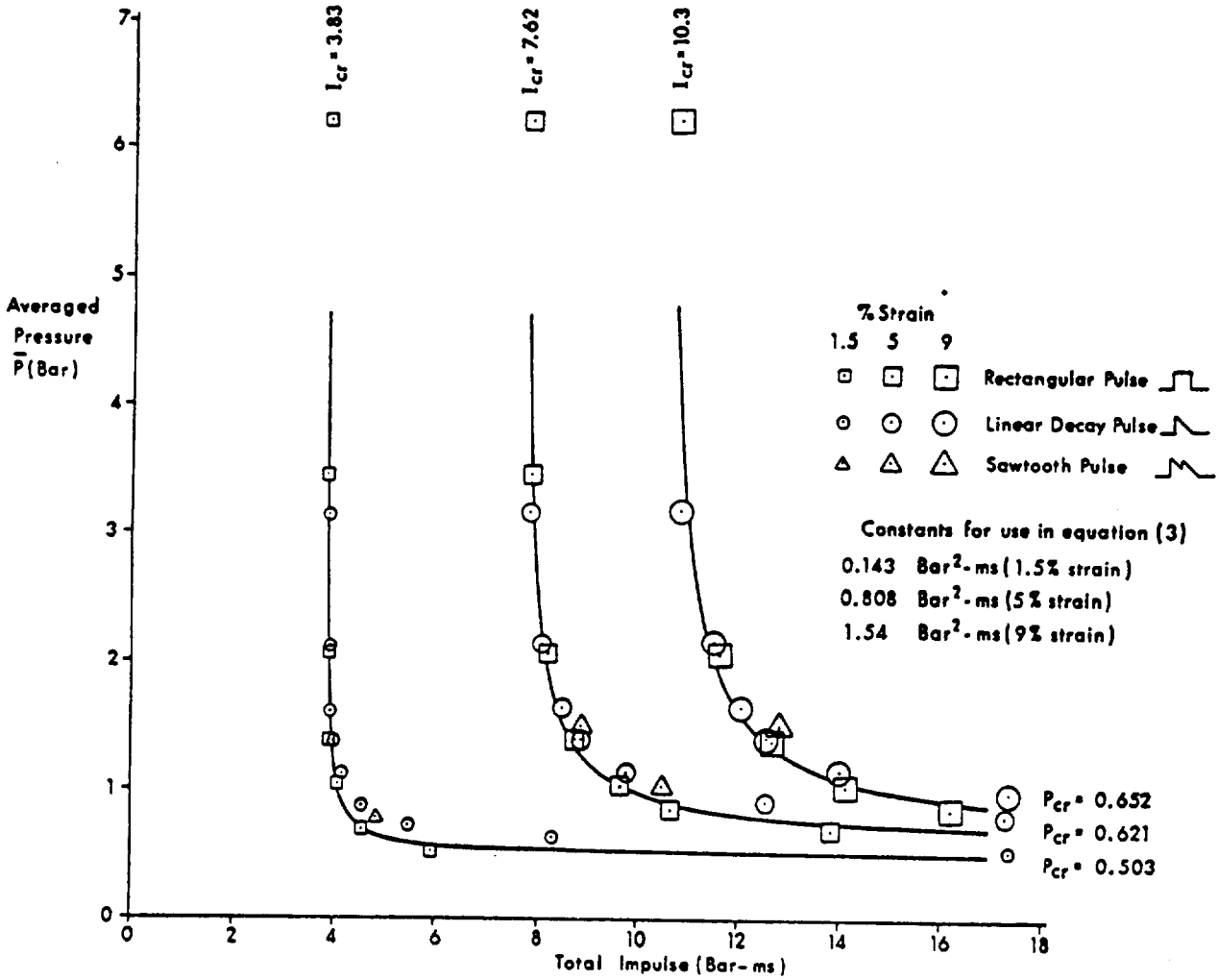

Figure 16. Plot of $\bar{P}$ Vs. Total Impulse for One Degree-of-Freedom Data.

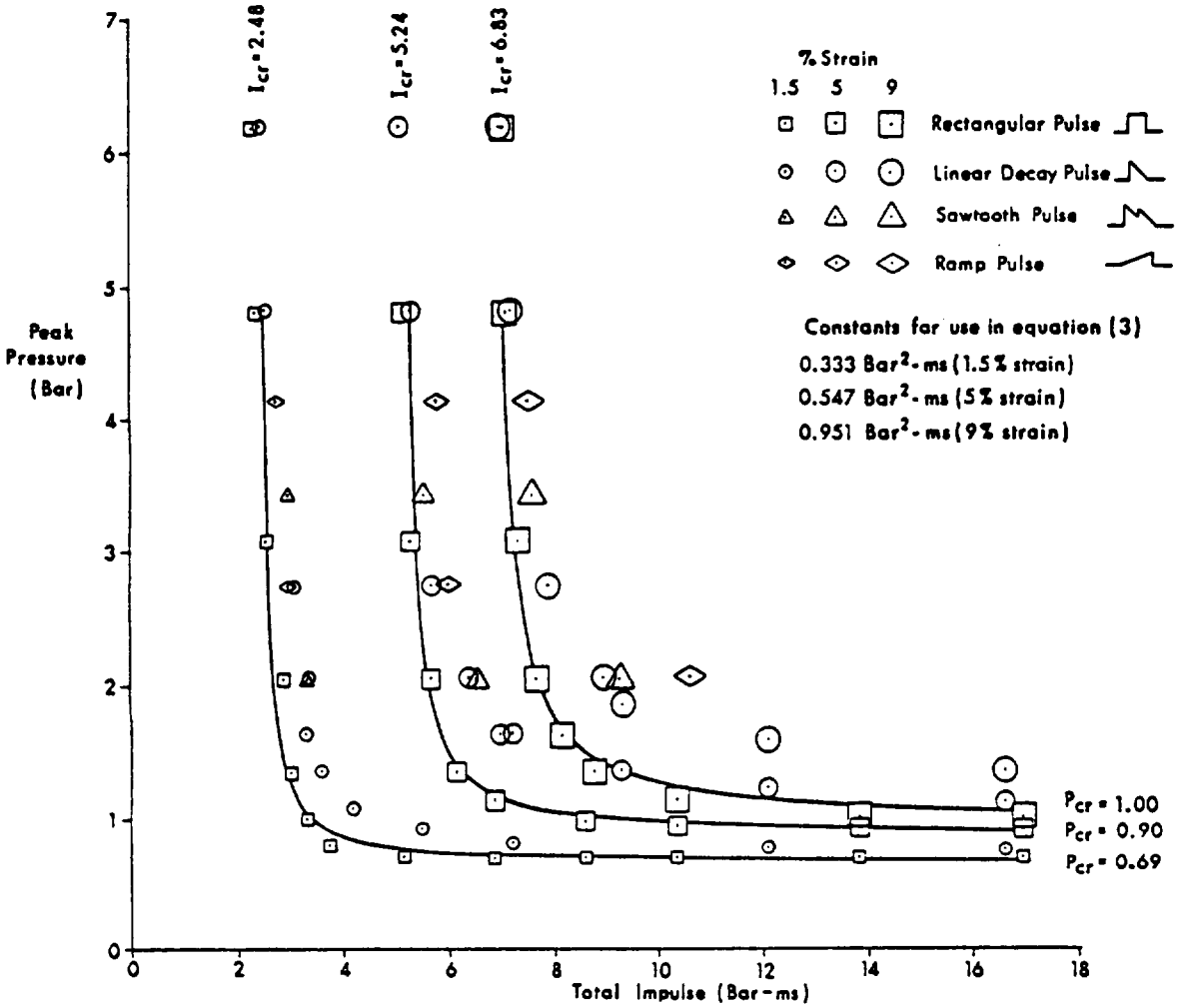

Figure 17. Plot of P_{peak} Vs. Total Impulse for Five Degree-of-Freedom Data.

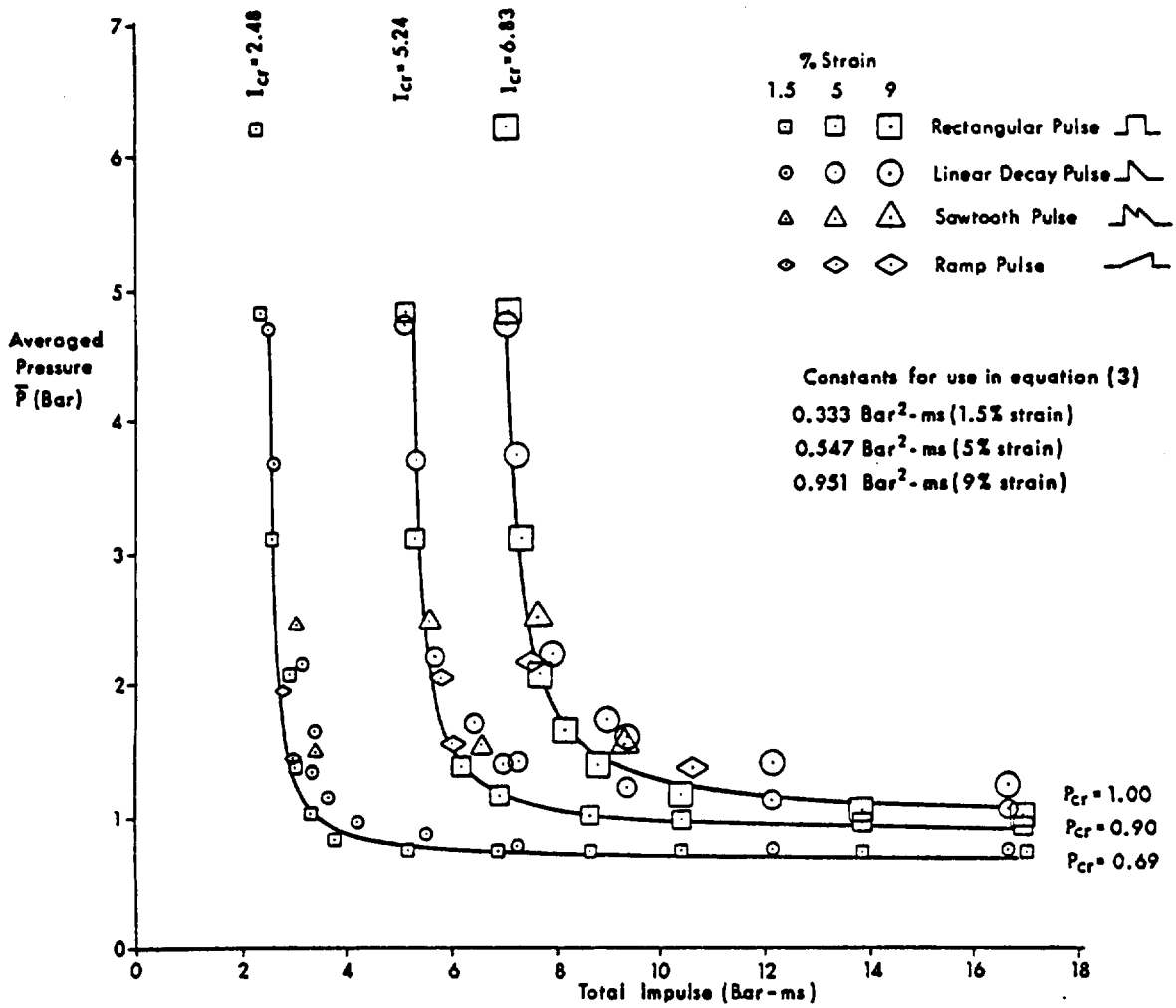

Figure 18. Plot of $\bar{P}$ Vs. Total Impulse for Five Degree-of-Freedom Data.

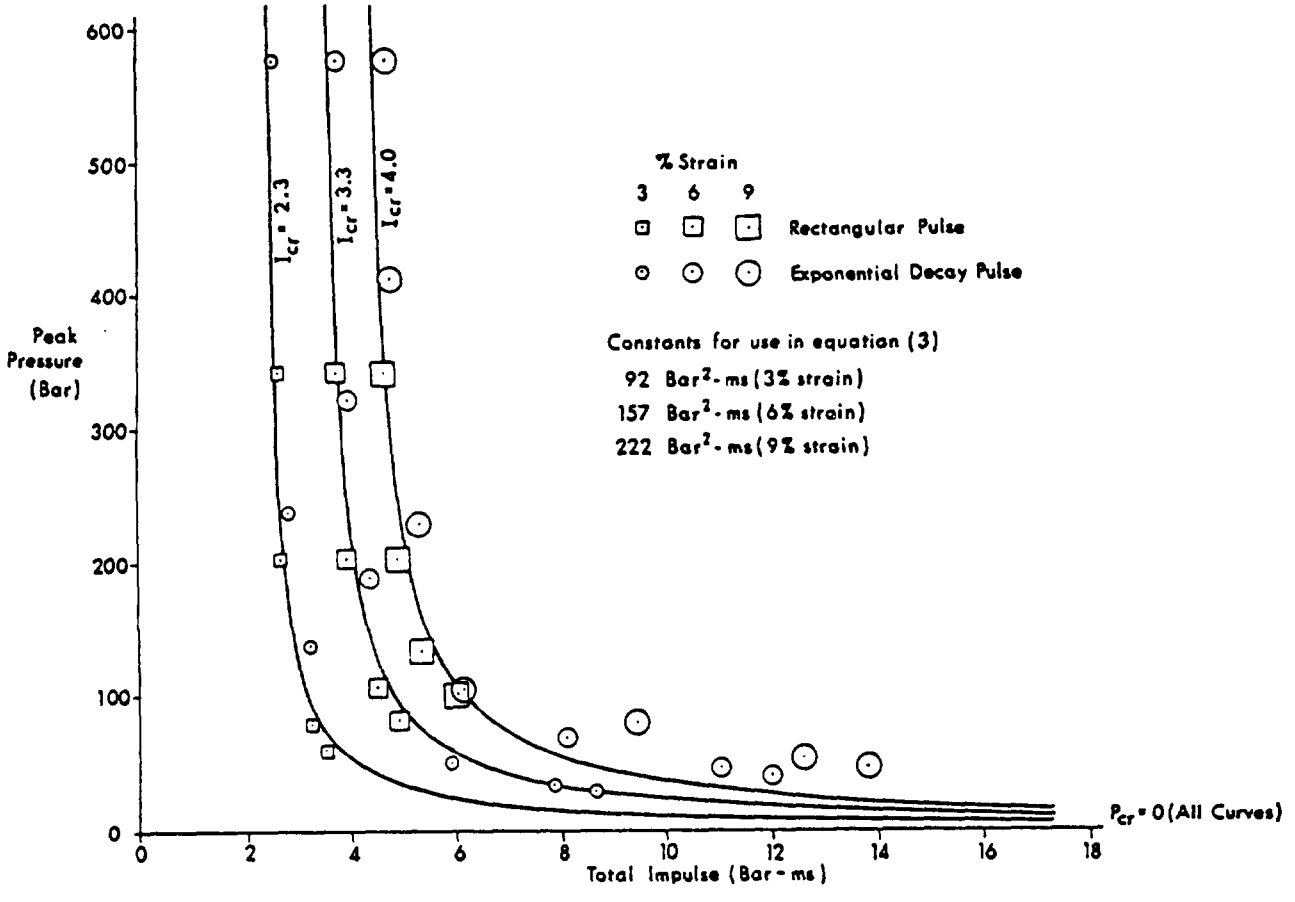

Figure 19. Plot of P_{peak} Vs. Total Impulse for REPSIL Data.

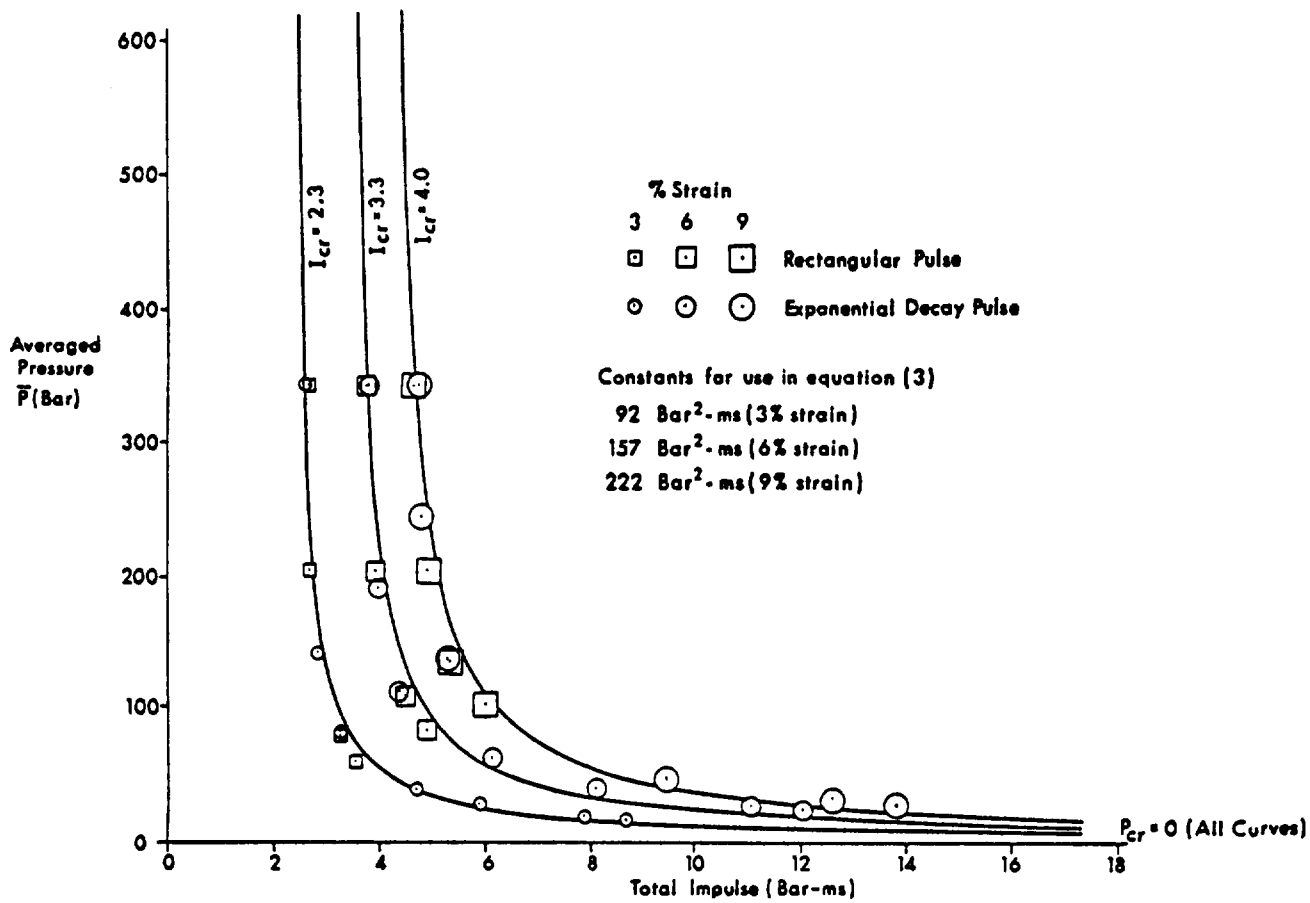

Figure 20. Plot of $\bar{P}$ Vs. Total Impulse for REPSIL Data.

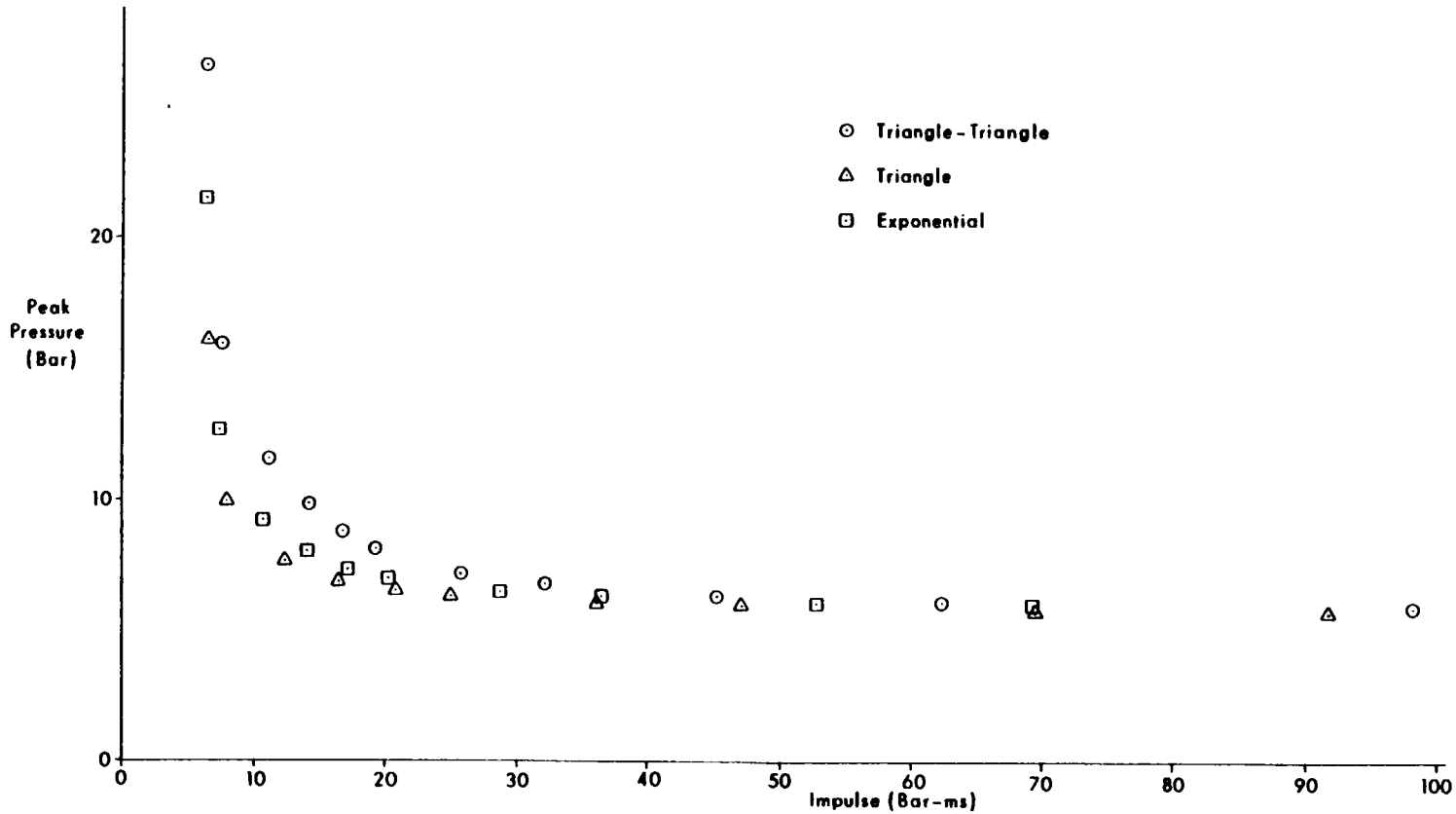

Figure 21. Plot of P_{peak} Vs. Total Impulse for Kaman 3 Percent Strain Data.

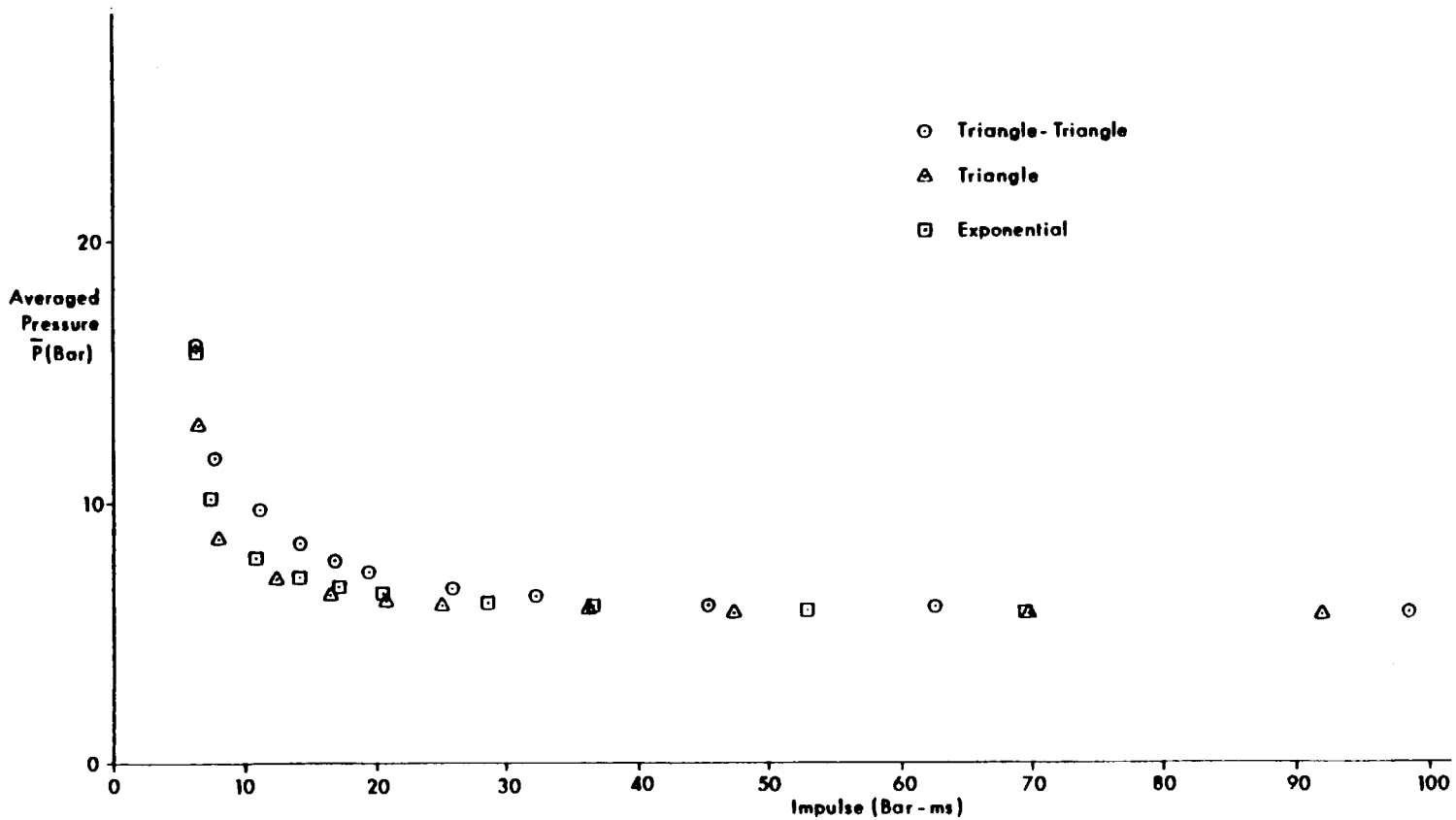

Figure 22. Plot of $\bar{P}$ Vs. Total Impulse For Kaman 3 Percent Strain Data.

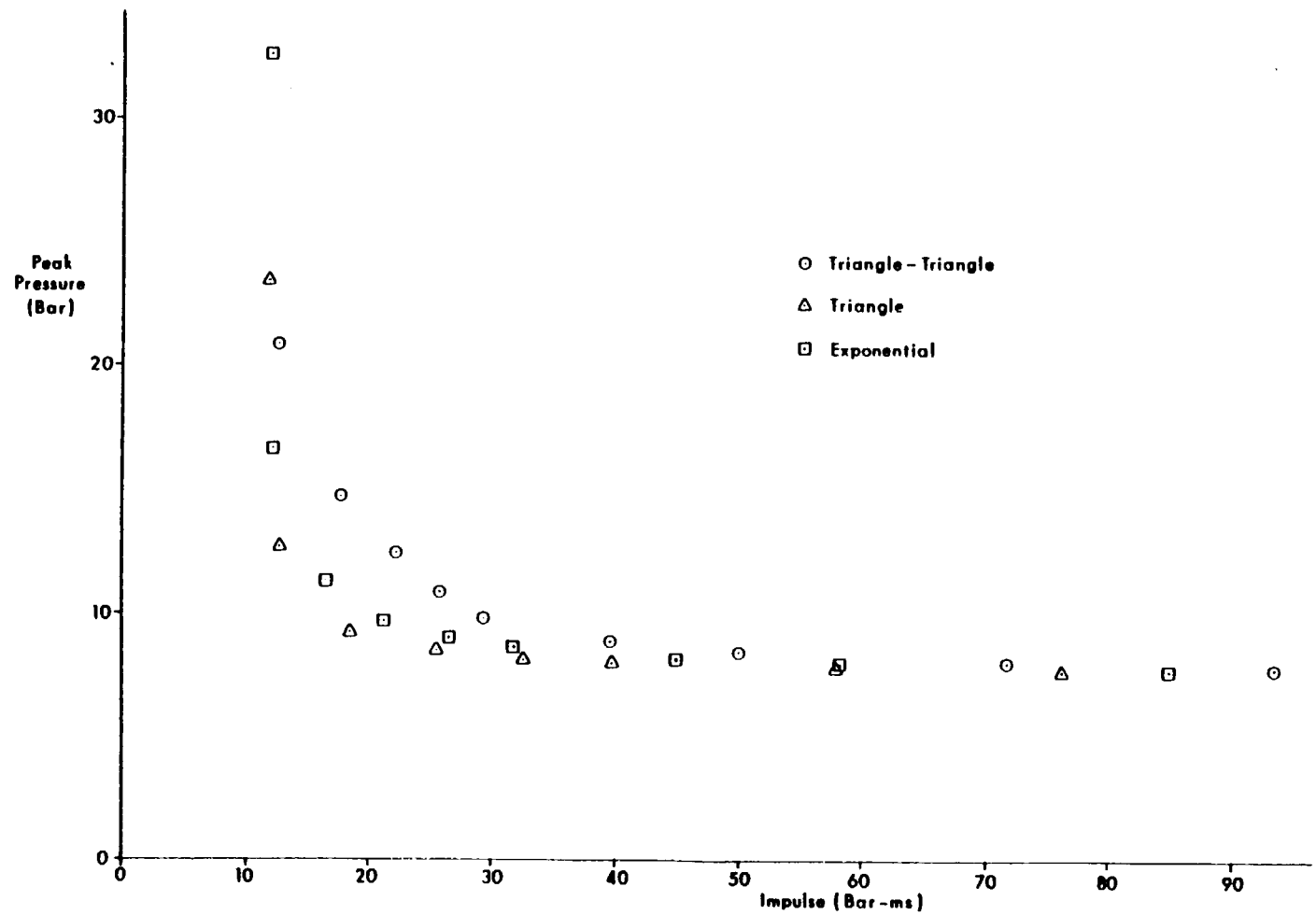

Figure 23. Plot of P_{peak} Vs. Total Impulse for Kaman 15 Percent Strain Data.

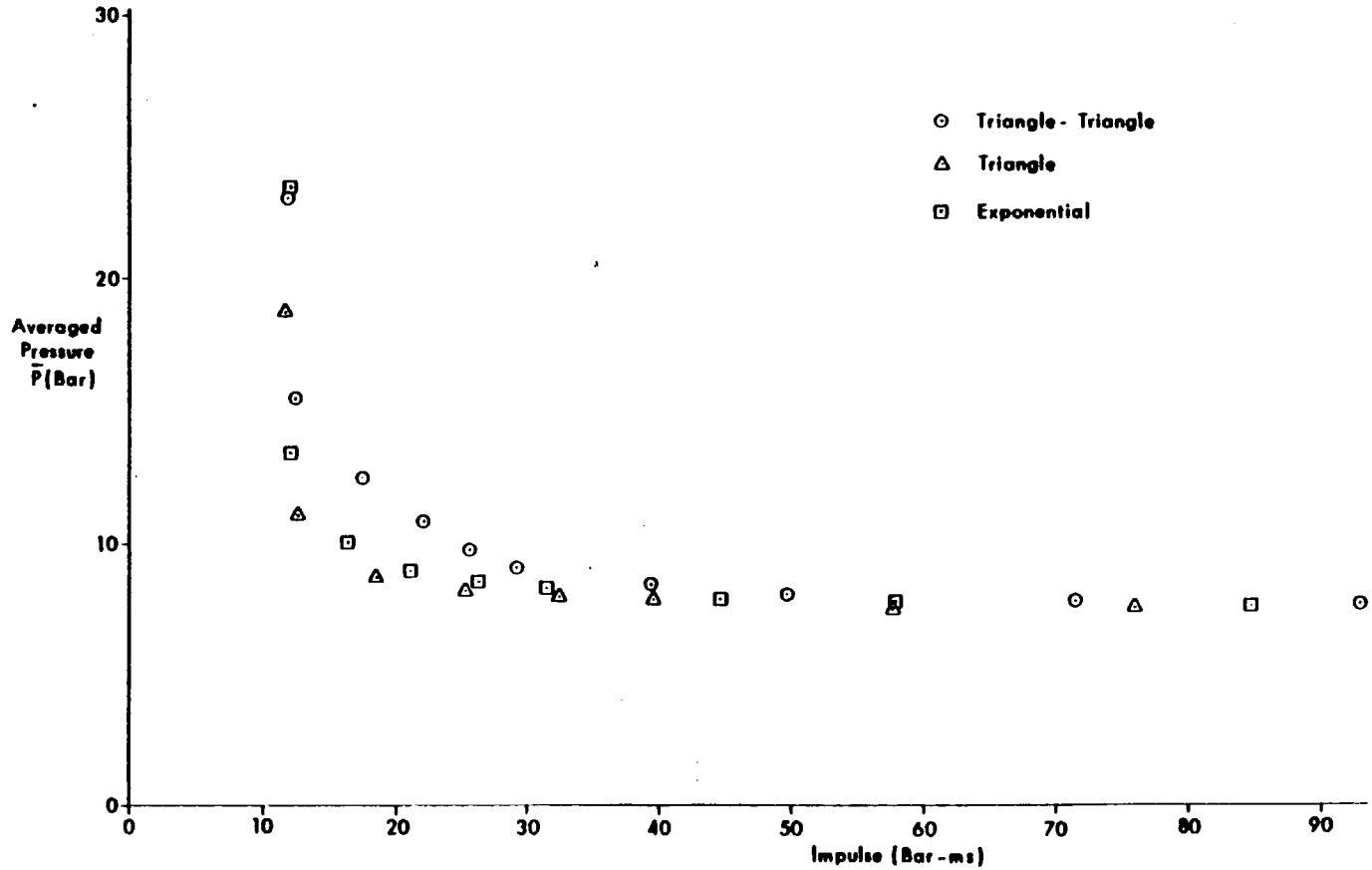

Figure 24. Plot of $\bar{P}$ Vs. Total Impulse for Kaman 15 Percent Strain Data.

for this position comes from the contractor data. This is a consequence of the strong similarity of the pulse shapes used (recall that all three are approximations to the same time history). No case shows the traditional method to be superior to the model proposed here.

VIII. SHOCK PULSE EFFECTIVENESS

In making comparisons of the pulses parameterized in Figures 6 and 14 one may ask: How are the traditional model

$$(P_{peak} - P_{cr})(I_{total} - I_{cr}) = K_t$$

and the proposed model

$$(\overline{P} - P_{cr})(I_{total} - I_{cr}) = K$$

related? Looking at Figure 6 one sees that $\overline{P}/P_{peak}$ is almost a linear function of P_{cr}/P_{peak}. Making use of this characteristic to approximate $\overline{P}/P_{peak}$ by

$$\frac{\overline{P}}{P_{peak}} = K_1 + (1 - K_1)\frac{P_{cr}}{P_{peak}}$$

we find that

$$\overline{P} = K_1 P_{peak} + (1 - K_1)P_{cr}$$

which may be substituted into the new iso-damage model with the result

$$(K_1 P_{peak} + P_{cr} - K_1 P_{cr} - P_{cr})(I_{total} - I_{cr}) = K$$

This simplifies to give

$$(P_{peak} - P_{cr})(I_{total} - I_{cr}) = \frac{K}{K_1} \quad .$$

Thus in the linear approximation to $\overline{P}/P_{peak}$ we find that the $P_{cr}/P_{peak} = 0$ intercept, K_1, is the transformation factor between the traditional and new models, i.e., $K_t = K/K_1$). In other words

$$K_1 * [(P_{peak} - P_{cr})(I_{total} - I_{cr})] = (\overline{P} - P_{cr})(I_{total} - I_{cr}) = K$$

Thus, we see that the proposed model is, in effect, a means of modifying the material contained in the traditional P-I maps. In general, it can be said that the parameter, K_1 is a quantitative measure of the effectiveness of a pulse as compared to a rectangular pulse having the same total impulse in causing damage irrespective of the target characteristics.

IX. USE OF THE PROPOSED MODEL IN DATA REDUCTION

So far, the discussion has been limited to the theoretical advantages of the present model. Another aspect which is of equal if not greater importance is that the proposed model is a practical tool for the reduction of test data. In short, the discussion so far has neglected objectives one and two of Section VI.

Figure 25 shows what we can expect to gather in the way of data from blast test instrumentation. As one can see, the loading is not classical. In applying methods that depend on peak pressures, total impulse and similarity to classical loading, the data reduction relies heavily on subjective judgement. With the proposed model, the results are integrals of time histories and as such are not dependent on subjective evaluation of empirical records. It will be possible to use the $\overline{P}$-I_{total} number pair or its derivative characterizations of the target response to a given attack in either theoretical or experimental studies.

Use of this model for data analysis should incur no additional cost because most agencies recording tests data now have the pressure-time histories digitized for computer plotting and impulse determination. Figure 25 provides a case in point. Data for two of five side-on pressure measurements taken on one Fuel Air Explosive (FAE) test are shown. The FAE device was initiated near the ground and identified as having a nominal charge weight of 33.6 kg.

In Figure 26 we see the damage number (DN) versus radius for this event. Also included on the figure are the damage numbers versus radius for bare spherical pentolite charges detonated in close proximity to the ground and assumed to have an effective charge weight of 1.8 times actual. The conclusion that we draw from this comparison is that for side-on pressure loading cases outside the cloud and near the ground, this FAE device is approximately 2.1 times as effective as Pentolite. This indicates that relatively soft targets can have damage numbers up to a limiting value as indicated by the knee in the curve.

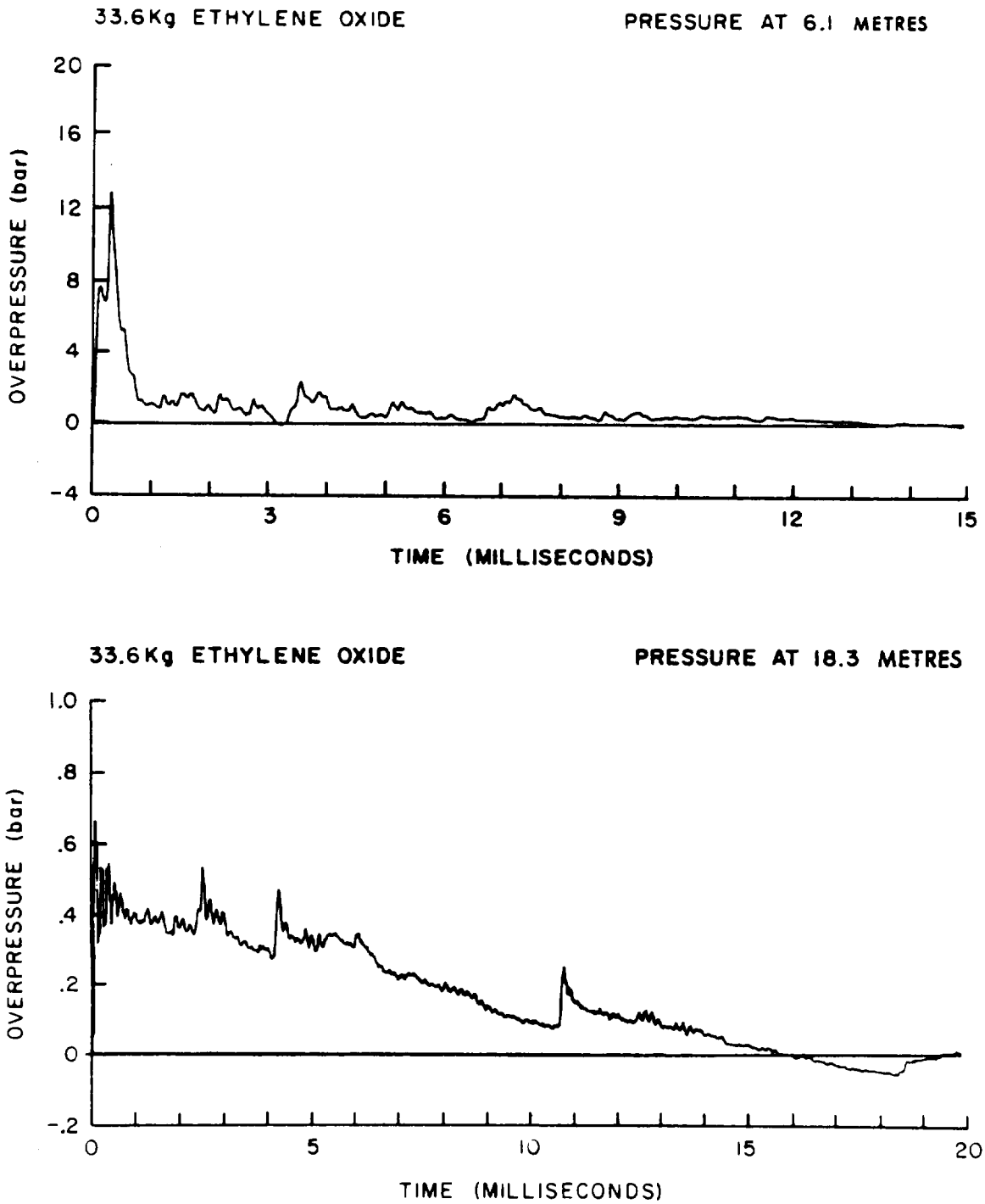

Figure 25. Typical Fuel-Air Explosive Pressure Time Histories.

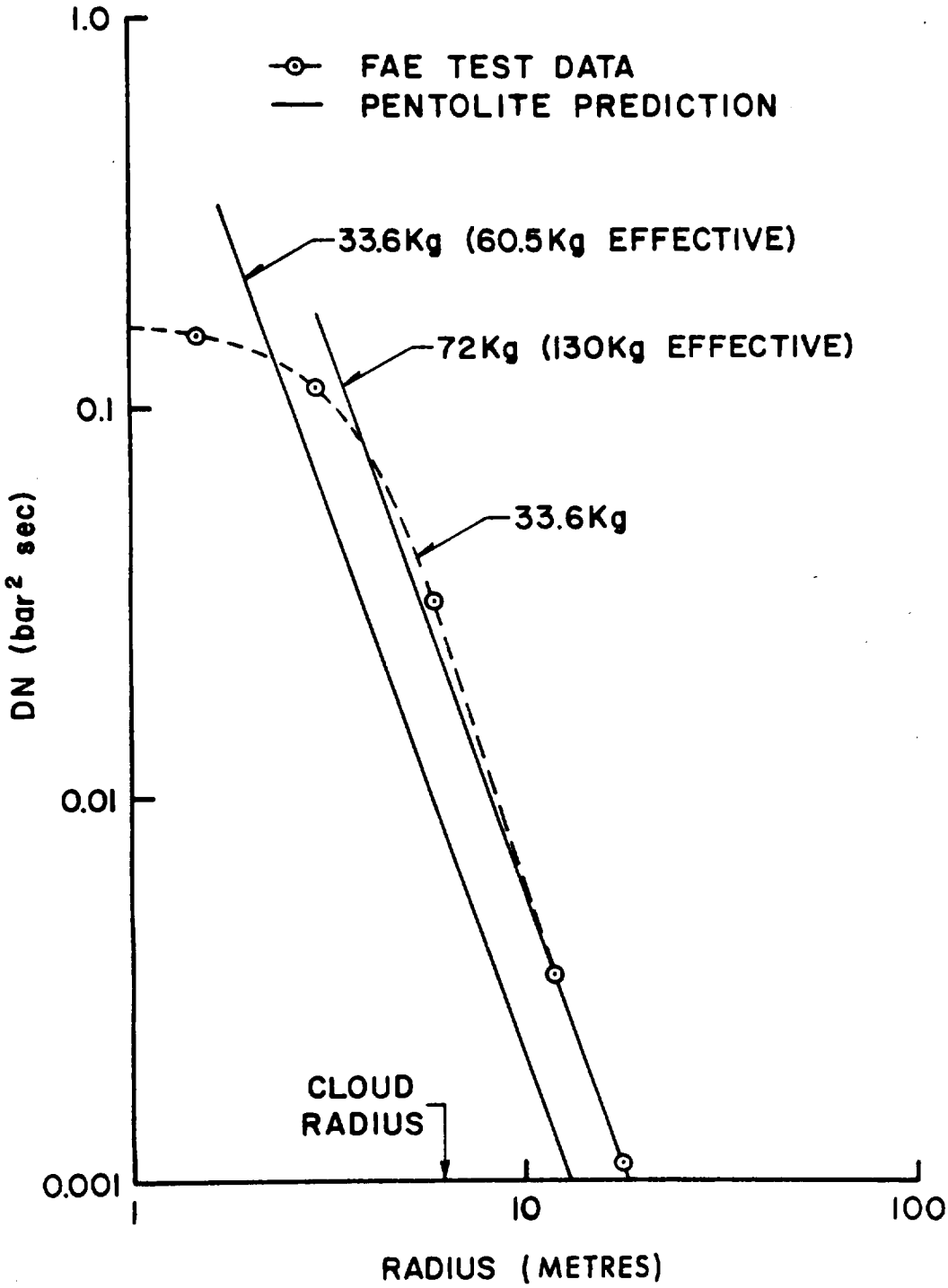

Figure 26. Damage Number Vs. Radius for Near Surface Bursts of Pentolite and Fuel-Air Explosive.

Another example of the use of this model in interpreting test data is shown in Figure 27. This figure shows localized loading time histories for two helicopters exposed to a large-scale high-explosive detonation.[11] The difference between the two curves results from one helicopter being revetted (lower curve) and the other one being unrevetted. One can see that the determination of the damaging potential of the loading functions (which, incidentially, for this case is a measure of the ability of the revetment to reduce damage) is enhanced as judged by use of the damage number criterion. Damage numbers for these two loading functions are included on the plots. It can be seen that the damage number for the non-revetted helicopter is slightly larger than that for the revetted helicopter. The ratios of the damage numbers (HELO 2/HELO 3) was found to be 1.14.

If one were to use the previous concepts for evaluating these same data, one would get a peak pressure ratio of 1.19, a total impulse ratio of 1.05 and a peak pressure-impulse product ratio of 1.26. These numbers indicate that the results would depend upon the ratio or ratios considered important. It is interesting to note that the average of these three ratios is 1.16, which is close to the ratio obtained using our model. It thus appears that our model can be of significant help in evaluating test results as well as in quantifying test data.

X. CONCLUSIONS

A conclusion which has been a defacto part of the blast community is that P-I methods are not applicable in the pure impulse and static load regions of dynamic structural response analysis. This conclusion has been brought into sharp focus by comparison of the presently proposed P-I method with its traditional and less versatile predecessor.

The proposed method provides an explanation for interesting previous methods having differing degrees-of-sophistication. These logical connections relate the one parameter method of O. T. Johnson to the two parameter P-I method. In turn, the P-I method is related to experiment and theory in structural blast damage.

The currently proposed method provides a convenient standard method of blast data reduction which may be applied to future experimental work and to correlate future data to that existing today.

The proposed method provides a means of relating damage from explosives having known characteristics to that caused by explosives having significantly different blast characteristics.

Finally, the present research has lead to an ongoing effort to apply statistical methods to validation of P-I iso-damage methodology.

---

[11] *R. N. Schumacher, "Blast Response of Helicopters Parked in Revetments (Event Mixed Company)," Ballistic Research Laboratories Memorandum Report No. 2516, August 1975, AD # B-006642-L.*

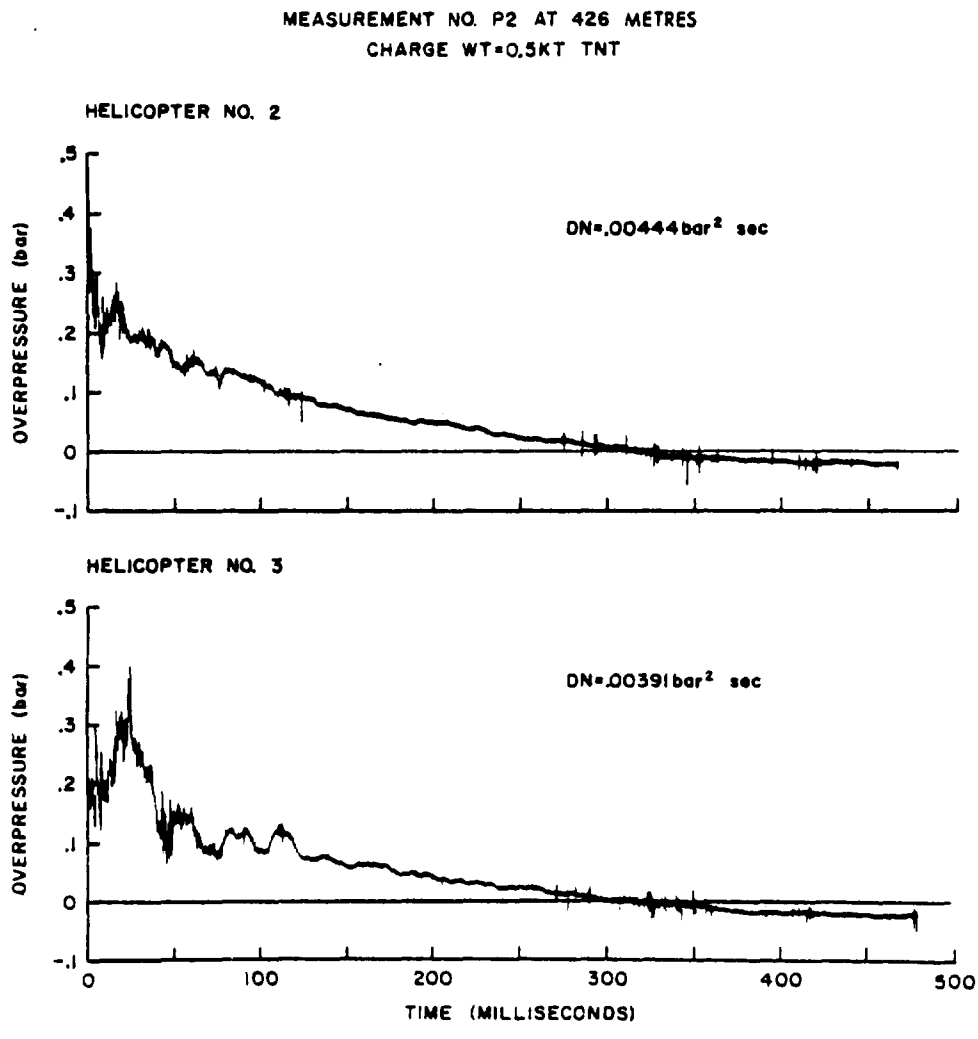

Figure 27. Pressure Loading Functions on Two Helicopters During a Large Scale Blast Field Trial.

REFERENCES

1. Wilfred E. Baker, Explosions in Air, Univ. of Texas Press, Austin, Texas, 1973.

2. F. B. Porzel, "Introduction to a Unified Theory of Explosions (UTE)," NOL TR-72-209, 14 September 1972, Unclassified.

3. J. Sperrazza, "Dependence of External Blast Damage to the A-25 Aircraft on Peak Pressure and Impulse," Ballistic Research Laboratories Memorandum Report 575, September 1951, AD # 378275.

4. O. T. Johnson, "A Blast-Damage Relationship," Ballistic Research Laboratories Report No. 1389, September 1967, AD # 388909.

5. C. K. Youngdahl, "Correlation Parameters for Eliminating the Effect of Pulse Shape on Dynamic Plastic Deformation," Journal of Applied Mechanics, pp. 744-752, September 1970.

6. H. J. Goodman, "Compiled Free-Air Blast Data on Bare Spherical Pentolite," Ballistic Research Laboratories Report No. 1092, February 1960, AD # 235278.

7. W. E. Baker, S. Silverman, P. A. Cox, Jr., and D. Young, "Structural Response of Helicopters to Muzzle and Breech Blast," Vol II, Final Technical Report SWRI 02-2029, Contract No. DAAD 05-67-C-0201 (BRL) dated March 1962.

8. N. J. Huffington, Jr., "Large Deflection Elastoplastic Response of Shell Structures," Ballistic Research Laboratories Report 1515, November 1970, AD # 717005.

9. N. J. Huffington, Jr., "An Analytical Study of Explosive Loading Techniques for Simulation of Impulsive Loading to Structures at Lethality Levels," Ballistic Research Laboratories Report No. 1621, November 1972, AD # 907436-L.

10. K. R. Wetmore, "An Interim Technical Report on Phase I of the BRL Pressure Impulse Blast Program," 30 September 1974, Contract DAA05-74-C-0742, Kaman Avidyne.

11. R. N. Schumacher, "Blast Response of Helicopters Parked in Revetments (Event Mixed Company)," Ballistic Research Laboratories Memorandum Report No. 2516, August 1975, AD # B-006642-L.

DISTRIBUTION LIST

No. of Copies	Organization
12	Commander Defense Documentation Center ATTN: DDC-TCA Cameron Station Alexandria, VA 22314
3	Director Defense Advanced Research Project Agency ATTN: Tech Lib NMRO PMO 1400 Wilson Boulevard Arlington, VA 22209
4	Director of Defense Research and Engineering ATTN: DD/TWP DD/S&SS DD/T&SS AD/SW Washington, DC 20301
2	Director Weapons Systems Evaluation Gp ATTN: CPT D. E. McCoy, USN Document Control Washington, DC 20305
1	Director Institute for Defense Analyses ATTN: IDA Librarian, Ruth S. Smith 400 Army-Navy Drive Arlington, VA 22202
2	Asst. to the Secretary of Defense (Atomic Energy) ATTN: Document Control Donald R. Cotter Washington, DC 20301
1	Office Secretary of Defense Office DDR&E ATTN: Mr. J. Persh, Staff Specialist Materials and Structures Washington, DC 20301
4	Director Defense Intelligence Agency ATTN: DT-1C/Dr. J. Vorona DI-7D/E. O. Farrell DT-2/Wpns & Sys Div Technical Library Washington, DC 20301
6	Director Defense Nuclear Agency ATTN: SPTD/Mr. J. Kelso SPSS/Dr. E. Sevin SPAS/Mr. J. Moulton STSP STVL/Dr. La Vier RATN/Cdr Alderson Washington, DC 20305
6	Director Defense Nuclear Agency ATTN: DDST/Mr. P. Hass DDST/Mr. M. Atkins STTL/Tech Lib (2 cy) STSI/Archives SPSS/LT J. R. Williams Washington, DC 20305
1	Commander Field Command, DNA ATTN: FCPR Kirtland AFB, NM 87115
1	Chief Las Vegas Liaison Office Field Command TD, DNA ATTN: Document Control P.O. Box 2702 Las Vegas, NV 89104

DISTRIBUTION LIST

No. of Copies	Organization
1	Commander Field Command, DNA Livermore Branch ATTN: FCPRL P. O. Box 808 Livermore, CA 94550
1	Director Defense Communications Agency ATTN: NMCSSC (Code 510) Washington, DC 20305
1	Director Joint Strategic Target Planning Staff JCS ATTN: Sci and Technical Information Lib Offutt AFB Omaha, NB 68113
2	Director National Security Agency ATTN: E. F. Butala, R154 P. E. Deboy, NSA 5232 Fort George G. Meade MD 20755
1	Commander US Army Materiel Development and Readiness Command ATTN: DRCDMA-ST 5001 Eisenhower Avenue Alexandria, VA 22333
1	Commander US Army Aviation Systems Command ATTN: DRSAV-E 12th and Spruce Streets St. Louis, MO 63166
1	Director US Army Air Mobility Research and Development Laboratory Ames Research Center Moffett Field, CA 94035
4	Commander US Army Electronics Command ATTN: DRSEL-RD DRSEL-TL-IR R. Freiberg J. Roma A. Sigismondi Fort Monmouth, NJ 07703
2	Commander US Army Missile Command ATTN: DRSMI-R Technical Library Redstone Arsenal, AL 35809
1	Commander US Army Missile Command ATTN: DRCPM-MDEI Redstone Arsenal, AL 35809
1	Commander US Army Tank Automotive Development Command ATTN: DRDTA-RWL Warren, MI 48090
2	Commander US Army Mobility Equipment Research and Development Command ATTN: Tech Docu Cen, Bldg. 315 DRSME-RZT Fort Belvoir, VA 22060

DISTRIBUTION LIST

No. of Copies	Organization
1	Commander US Army Armament Command ATTN: SARRI-LR/Mr. B. Morris Rock Island, IL 61202
1	Commander US Army Picatinny Arsenal ATTN: SARPA-V Mr. G. Demitrack Dover, NJ 07801
1	Commander US Army White Sands Missile Range ATTN: STEWS-TE-N/Mr. J. Gorman White Sands, NM 88002
1	Commander US Army Rock Island Arsenal Rock Island, IL 61202
1	Commander US Army Watervliet Arsenal Watervliet, NY 12189
5	Commander US Army Harry Diamond Labs ATTN: DRXDO-TI DRXDO-TI/012 Mr. F. N. Wimenitz Mr. Jim Gaul DRXDO-NP Mr. J. Gwaltney DRXDO-RBH Mr. P. A. Caldwell 2800 Powder Mill Road Adelphi, MD 20783
1	Commander US Army Materials and Mechanics Research Center ATTN: Technical Library Watertown, MA 02172
1	Commander US Army Natick Research and Development Center ATTN: DRXRE/Dr. D. Sieling Natick, MA 01762
1	Commander US Army Foreign Science and Technology Center ATTN: Rsch & Data Branch Federal Office Building 220 7th Street, NE Charlottesville, VA 22901
1	Director US Army TRADOC Systems Analysis Activity ATTN: ATAA-SA White Sands Missile Range NM 88002
3	Commander US Army Nuclear Agency ATTN: ATCN-W/CPT Ader CDINS-E Technical Library Fort Bliss, TX 79916
1	Commander US Army Communications Command ATTN: Technical Library Fort Huachuca, AZ 85613
1	Interservice Nuclear Weapons School ATTN: Technical Library Kirtland AFB, NM 87115
2	HQDA (DAMA-AR; NCB Div) Washington, DC 20310
2	HQDA (DAEN-MC; DAEN-CWE) Washington, DC 20310

DISTRIBUTION LIST

No. of Copies	Organization
2	Department of the Army Office, Chief of Engineers Publications Department ATTN: DAEN-MCE-D DAEN-RDM 890 South Pickett Street Alexandria, VA 22304
3	Director US Army Advanced BMD Technology Center ATTN: CRDABH-X/J. Davidson CRDABH-S/Mr. M. Capps N. J. Hurst Huntsville, AL 35807
1	Commander US Army Research Office P.O. Box 12211 Research Triangle Park NC 27709
4	Commander US Army Engineer Waterways Experiment Station ATTN: Technical Library William Flathau John N. Strange James Ballard P.O. Box 631 Vicksburg, MS 39180
2	Director Defense Civil Preparedness Agency ATTN: Mr. George Sisson/RF-SR Technical Library Washington, DC 20301
1	Commander US Army Engineering Center ATTN: ATSEN-SY-L Fort Belvoir, VA 22060
1	Director US Army Construction Engineering Research Laboratory ATTN: CERL-SL P.O. Box 4005 Champaign, IL 61820
1	Division Engineer US Army Engineering Division ATTN: Docu Cen Ohio River P.O. Box 1159 Cincinnati, OH 45201
1	Division Engineer US Army Engineering Division ATTN: Mr. M. Dembo Huntsville Box 1600 Huntsville, AL 35804
5	Chief of Naval Research ATTN: Code 464/Jacob L. Warner Code 464/Thomas P. Quinn N. Perrone (2 cy) Technical Library Department of the Navy Washington, DC 20360
2	Chief of Naval Operations ATTN: OP-03EG OP-985F Department of the Navy Washington, DC 20350
1	Chief of Naval Material ATTN: MAT 0323 Department of the Navy Arlington, VA 22217
1	Director Strategic Systems Project Ofc ATTN: NSP-43, Tech Lib Department of the Navy Washington, DC 20360

DISTRIBUTION LIST

No. of Copies	Organization
1	Commander US Naval Electronic Systems Command ATTN: PME 117-21A Washington, DC 20360
2	Commander US Naval Sea Systems Command ATTN: ORD-91313 Library Code 03511 Department of the Navy Washington, DC 20362
1	Commander US Naval Facilities Engineering Command ATTN: Code 03A Code 04B Technical Library Washington, DC 20360
3	Officer-in-Charge US Naval Civil Engineering Laboratory Naval Construction Battalion Center ATTN: Stan Takahashi R. J. Odello Technical Library Port Hueneme, CA 93041
2	Commander US Naval Ship Engineering Center ATTN: Tech Library NSEC 6105G Hyattsville, MD 20782
1	Commander US David W. Taylor Naval Ship Research and Development Center ATTN: L42-3 Library Bethesda, MD 20084
1	Commander US Naval Surface Weapons Center ATTN: Technical Library Dahlgren, VA 22448
3	Commander US Naval Surface Weapons Center ATTN: Code 1224/Navy Nuclear Programs Office Code 730/Tech Lib Francis B. Porzel Silver Spring, MD 20910
2	Commander US Naval Ship Research and Development Center Facility Underwater Explosions Rsch Div ATTN: Code 17/W.W. Murray Technical Library Portsmouth, VA 23709
1	Commander US Naval Weapons Evaluation Facility Kirtland AFB Albuquerque, NM 87117
2	Commander and Director US Naval Civil Engineer Lab ATTN: Code L31/Mr. Shaw Mr. R. Siebold Port Hueneme, CA 93041
2	Commander US Naval Research Laboratory ATTN: Code 2027/Tech Lib Code 8440/F. Rosenthal Washington, DC 20375
1	Superintendent US Naval Postgraduate School ATTN: Code 2124/Tech Rpts Lib Monterey, CA 93940

DISTRIBUTION LIST

No. of Copies	Organization
1	HQ USAF (SAFRD) Washington, DC 20330
1	HQ USAF (INATA) Washington, DC 20330
1	HQ USAF (PRF) Washington, DC 20330
2	AFSC (DLCAW; Tech Lib) Andrews AFB Washington, DC 20331
2	AFATL (ATRD/R. Brandt) Eglin AFB, FL 32542
1	RADC (FMTLD/Docu Lib) Griffiss AFB, NY 13340
1	AFSWC (SWTSX) Kirtland AFB, NM 87117
1	AFWL (SUL) Kirtland AFB, NM 87117
3	AFWL (Robert Port; DEV Jimmie L. Bratton; DEV M. A. Plamondon) Kirtland AFB, NM 87117
1	Commander-in-Chief Strategic Air Command ATTN: NRI-STINFO Lib Offut AFB, NB 68113
1	AFML (MAMD/Dr. T. Nicholas) Wright-Patterson AFB OH 45433
1	FTD (TDPTN) Wright-Patterson AFB OH 45433
1	AFIT (Lib Bldg. 640, Area B) Wright-Patterson AFB OH 45433
1	Director US Bureau of Mines ATTN: Technical Library Denver Federal Center Denver, CO 80225
1	Director US Bureau of Mines Twin Cities Research Center ATTN: Technical Library P.O. Box 1660 Minneapolis, NM 55111
1	US Energy Research and Development Administration Division of Headquarters Svcs ATTN: Doc Control for Classified Tech Lib Library Branch G-043 Washington, DC 20545
1	US Energy Research and Development Administration Albuquerque Operations Office ATTN: Doc Control for Tech Lib P.O. Box 5400 Albuquerque, NM 87115
1	US Energy Research and Development Administration Nevada Operations Office ATTN: Doc Control for Tech Lib P.O. Box 14100 Las Vegas, NV 89114
2	Director Lawrence Livermore Laboratory ATTN: Larry W. Woodruff, L-125 Technical Information Div P.O. Box 808 Livermore, CA 94550

DISTRIBUTION LIST

No. of Copies	Organization
1	Director Los Alamos Scientific Lab ATTN: Doc Control for Rpt Lib P.O. Box 1663 Los Alamos, NM 87544
1	Director NASA Scientific and Tech Info Facility ATTN: SAK/DL P.O. Box 8757 Baltimore/Washington International Airport, MD 21240
1	National Academy of Sciences ATTN: Mr. D. G. Groves 2101 Constitution Avenue, NW Washington, DC 20418
1	Agbabian Associates ATTN: M. Agbabian 250 North Nash Street El Segundo, CA 90245
2	Applied Theory, Inc. ATTN: John G. Trulio 1010 Westwood Blvd. Los Angeles, CA 90024
1	AVCO Government Products Group ATTN: Res Lib A830, Rm 7201 201 Lowell Street Wilmington, MA 01887
1	AVCO Corporation Structures and Mechanics Dept. ATTN: Dr. William Broding Mr. J. Gilmore Wilmington, MA 01887
1	The BDM Corporation ATTN: Technical Library 1920 Aline Avenue Vienna, VA 22180
1	Bell Telephone Labs, Inc, ATTN: Tech Rpt Ctr Mountain Avenue Murray Hill, NJ 07971
1	The Boeing Company ATTN: Aerospace Library P.O. Box 3707 Seattle, WA 98124
2	California Research and Technology, Inc. ATTN: Ken Kreyenhagen Technical Library 6269 Variel Avenue Woodland Hills, CA 91364
1	Calspan Corporation ATTN: Technical Library P.O. Box 235 Buffalo, NY 14221
1	Civil/Nuclear Systems Corporation ATTN: Robert Crawford 1200 University N.E. Albuquerque, NM 87102
1	EG&G, Incorporated Albuquerque Division ATTN: Technical Library P.O. Box 10218 Albuquerque, NM 87114
1	General American Trans Corporation General American Research Division ATTN: G. L. Neidhardt 7449 N. Matchez Avenue Niles, IL 60648
1	General Electric Company-TEMPO ATTN: DASIAC P.O. Drawer QQ Santa Barbara, CA 93102

DISTRIBUTION LIST

No. of Copies	Organization
1	President General Research Corporation ATTN: Library McLean, VA 22101
1	J. G. Engineering Research Associates 3831 Menlo Drive Baltimore, MD 21215
1	J. L. Merritt Consulting & Special Engineering Services, Inc. ATTN: Technical Library P.O. Box 1206 Redlands, CA 92373
2	Kaman AviDyne ATTN: Dr. N. P. Hobbs Mr. S. Criscione 83 Second Avenue Northwest Industrial Park Burlington, MA 01803
2	Kaman Sciences Corporation ATTN: Library Dr. Don Sachs 1500 Garden of the Gods Road Colorado Springs, CO 80907
2	Lockheed Missiles & Space Co. ATTN: T. Gerrs D/52-33, Bldg. 205 Tech Info Ctr,Doc/Coll. 3251 Hanover Street Palo Alto, CA 94304
1	McDonnell Douglas Corporation ATTN: Robert W. Halprin 5301 Bolsa Avenue Huntington Beach, CA 92647
1	Honeywell, Inc. Govt & Aero Products Div 600 Second Street N.E. Hopkins, MN 55343
1	The Mitre Corporation ATTN: Library RT 62 and Middlesex Turnpike P.O. Box 208 Bedford, MA 01730
2	Physics International Corp. ATTN: E. T. Moore Dennis Orphal 2700 Merced Street San Leandro, CA 94577
4	Physics International Corp. ATTN: Robert Swift Charles Godfrey Larry A. Behrmann Technical Library 2700 Merced Street San Leandro, CA 94577
5	R&D Associates ATTN: Dr. H. L. Brode Dr. Albert L. Latter Bruce Hartenbaum William B. Wright Henry Cooper P.O. Box 9695 Marina del Rey, CA 90291
4	R&D Associates ATTN: Jerry Carpenter Sheldon Schuster J. G. Lewis Technical Library P.O. Box 9695 Marina del Rey, CA 90291
1	Sandia Laboratories ATTN: Doc Control for 3141 Sandia Report Coll. P.O. Box 5800 Albuquerque, NM 87115
1	John Hindes, Consultant P.O. Box 6434 Santa Barbara, CA 93111

DISTRIBUTION LIST

No. of Copies	Organization
2	Sandia Laboratories Livermore Laboratory ATTN: Doc Control for Tech Lib Doc Control for L. Hill P.O. Box 969 Livermore, CA 94550
1	Electromechanical Systems of New Mexico, Inc. ATTN: R.A.Shunk PO Box 11730 Albuquerque, NM 87112
3	Science Applications, Inc. ATTN: R. Seebaugh William M. Layson John Mansfield 1651 Old Meadow Road McLean, VA 22101
2	Science Applications, Inc. ATTN: David Bernstein D. E. Maxwell 7850 Edgewater Drive Oakland, CA 94621
2	Science Applications, Inc. ATTN: Technical Library Michael McKay P.O. Box 2351 LaJolla, CA 92038
1	Shock Hydrodynamics, Inc. A Division of Whittaker Corp. ATTN: L. Zernow 4710-16 Vineland Avenue North Hollywood, CA 91602
5	Systems, Science & Software ATTN: Robert T. Allen Donald R. Grine Ted Cherry Thomas D. Riney Technical Library P.O. Box 1620 La Jolla, CA 92037
2	Terra Tek, Inc. ATTN: Sidney Green Technical Library 420 Wakara Way Salt Lake City, UT 84108
2	Tetra Tech, Inc. ATTN: Li-San Hwang Technical Library 630 North Rosemead Blvd. Pasadena, CA 91107
7	TRW Systems Group ATTN: Paul Lieberman Benjamin Sussholtz Norm Lipner William Rowan Jack Farrell Pravin Bhutta Tech Info Ctr/S-1930 One Space Park Redondo Beach, CA 90278
2	TRW Systems Group ATTN: Mr. F. A. Pieper Greg Hulcher San Bernardino Operations P.O. Box 1310 San Bernardino, CA 92402
2	Union Carbide Corporation Holifield National Laboratory ATTN: Doc Control for Tech Lib Divil Defense Research Proj. P.O. Box X Oak Ridge, TN 37830
1	Universal Analytics, Inc. ATTN: E. I. Field 7740 W. Manchester Blvd. Playa Del Rey, CA 90291

DISTRIBUTION LIST

No. of Copies	Organization
1	URS Research Company ATTN: Technical Library 155 Bovet Road San Mateo, CA 94402
1	Weidlinger Assoc. Consulting Engineers ATTN: J. Isenbert 2710 San Hill Road Suite 230 Menlo Park, CA 99025
1	Westinghouse Electric Company Marine Division ATTN: W. A. Volz Hendy Avenue Sunnyvale, CA 94008
1	Battelle Memorial Institute ATTN: Technical Library 505 King Avenue Columbus, OH 43201
4	Denver Research Institute University of Denver ATTN: Mr. J. Wisotski Fred P. Vanditti Ron W. Buchanon Technical Library P.O. Box 10127 Denver, CO 80210
3	IIT Research Institute ATTN: Milton R. Johnson R. E. Welch Technical Library 10 West 35th Street Chicago, IL 60616
2	Lovelace Foundation for Medical Education ATTN: Asst Dir of Research/ Robert K. Jones Technical Library 5200 Gibson Blvd, SE Albuquerque, NM 87108
1	Massachusetts Institute of Technology Aeroelastic and Structures Research Laboratory ATTN: Dr. E. A. Witmer Cambridge, MA 02139
2	Southwest Research Institute ATTN: Dr. W. E. Baker A. B. Wenzel 8500 Culebra Road San Antonio, TX 78206
4	Stanford Research Institute ATTN: Dr. G. R. Abrahamson Carl Peterson Burt R. Gasten SRI Library, Rm G021 333 Ravenswood Avenue Menlo Park, CA 94025
1	University of California Berkeley Campus, Rm 8 ATTN: G. Sackman 2543 Channing Way Berkeley, CA 94720
1	University of Dayton ATTN: Hallock F. Swift 300 College Park Avenue Dayton, OH 45409
1	University of Illinois Consulting Engineering Services ATTN: Nathan M. Newmark 1114 Civil Engineering Building Urgana, IL 61801
2	The University of New Mexico The Eric H. Wang Civil Engineering Research Facility ATTN: Larry Bickle Neal Baum University Station Box 188 Albuquerque, NM 87131

DISTRIBUTION LIST

No. of Copies	Organization
2	Washington State University Administration Office ATTN: Arthur Miles Hohorf George Duval Pullman, WA 99163

Aberdeen Proving Ground

Marine Corps Ln Ofc
Dir, USAMSAA
ATTN: Dr. J. Sperrazza
Mr. R. Norman, GWD
Dr. Rivello
R. Bailey